

**UNIVERSITY OF TURKISH AERONAUTICAL ASSOCIATION
INSTITUTE OF SCIENCE AND TECHNOLOGY**

**DESIGN AND IMPLEMENTATION OF AN ENHANCED
WIRELESS POWER TRANSFER SYSTEM**



Master Thesis

Khalid Waleed Hussein AL-HASHEMI

**INSTITUTE OF SCIENCE AND TECHNOLOGY
ELECTRICAL AND ELECTRONICS ENGINEERING DEPARTMENT**

DECEMBER, 2017

**UNIVERSITY OF TURKISH AERONAUTICAL ASSOCIATION
INSTITUTE OF SCIENCE AND TECHNOLOGY**

**DESIGN AND IMPLEMENTATION OF AN ENHANCED
WIRELESS POWER TRANSFER SYSTEM**



Master Thesis

Khalid Waleed Hussein AL-HASHEMI

1406030014

**IN PARTIAL FULFILLMENT OF THE REQUIREMENT FOR THE
DEGREE OF MASTER OF SCIENCE IN ELECTRICAL ENGINEERING**

Thesis Supervisor: Prof. Dr. Dođan ALIKOĐLU

Khalid Waleed Hussein Al-Hashemi, having student number 1406030014 and enrolled in the Master Program at the Institute of Science and Technology at the University of Turkish Aeronautical Association, after meeting all of the required conditions contained in the related regulations, has successfully accomplished, in front of jury, the presentation of the thesis prepared with the title of: "Design and Implementation Of An Enhanced Wireless Power Transfer System"

Supervisor : Prof. Dr. Dođan ALIKOĐLU
University of Turkish Aeronautical Association

Jury Members : Prof. Dr. Dođan ALIKOĐLU
University of Turkish Aeronautical Association

: Assoc. Prof. Dr. Ahmet KARAARSLAN
Yildirim Beyazit University

: Assist. Prof. Javad RAHEBI
University of Turkish Aeronautical Association

Thesis Defense Date: 12.12.2017

**THE UNIVERSITY OF TURKISH AERONAUTICAL ASSOCIATION
INSTITUTE OF SCIENCE AND TECHNOLOGY**

I hereby declare that all the information in this study I presented as my Master's Thesis, called "Design And Implementation of an Enhanced Wireless Power Transfer System" has been presented in accordance with the academic rules and ethical conduct. I also declare and certify on my honor that I have fully cited and referenced all the sources I made use of in this present study.



12/12/2017

Khalid AL-HASHEMI

ACKNOWLEDGEMENTS

I am grateful to The Almighty GOD for helping me by giving me the strength to complete this thesis.

I would like to acknowledge my late grandfather who had such a huge impact on my life.

I would like to thank my parents and my wife for supporting me throughout my academic study. Without their moral support, interest and encouragement for my academic work, the completion of this effort would not have been possible.

I would like to acknowledge my beautiful four children who make my life worthwhile.

I would like to express my sincere gratitude to Prof. Dr. Dođan ALIKOĐLU at the University of Turkish Aeronautical Institute for his sound advice and constructive criticisms in the evaluation of the results. He has helped me in this project and has willingly shared his knowledge and ideas with me.

December 2017

Khalid AL-HASHEMI

TABLE OF CONTENTS

ACKNOWLEDGEMENTS	iv
TABLE OF CONTENTS	v
LIST OF TABLES	vii
LIST OF FIGURES	viii
LIST OF ABBREVIATIONS	x
ABSTRACT	xi
ÖZET	xii
CHAPTER ONE	1
1. INTRODUCTION	1
1.1 Presentation of the Work	1
1.2 Wireless Power Transfer	1
1.2.1 The Importance of WPT and Its Applications	2
1.2.2 Types of WPT Systems and Their Properties	3
1.3 Literature Survey	5
1.4 Motivation	8
1.5 Main Aspect of the Work	9
1.6 Thesis Layout	10
CHAPTER TWO	11
2. THEORETICAL GROUNDS FOR WIRELESS POWER TRANSFER	11
2.1 Overview of an Inductive Power Transfer System.....	11
2.2 Mutual Inductance Concepts and Coupling Coefficient.....	12
2.3 Equivalent Series Resistance of the Coils and Quality Factor	15
2.4 The Equivalent Circuit.....	17
2.5 Resonant Inductive Coupling	18
CHAPTER THREE	19
3. BLOCK DIAGRAM REPRESENTATION OF THE WPT SYSTEM AND ITS COMPONENTS	19
3.1 Introduction	19
3.2 Block Diagram of the Wireless Power Transfer System.....	19
3.2.1 DC Power Supply Source	20
3.2.2 DC Regulator I.....	20
3.2.3 Pulse Generator	21
3.2.4 DC/AC Converter	21
3.2.5 Transmitter Coil.....	21
3.2.6 Receiver Coil	21
3.2.7 AC/DC Converter	21
3.2.8 DC Regulator II.....	22
3.2.9 The Load	22
3.3 The Components.....	22
3.3.1 Diodes	22

3.3.1.1	Zener diode.....	23
3.3.1.2	Schottky diode.....	24
3.3.1.3	Diode bridge rectifier.....	24
3.3.1.4	Light emitting diode (LED).....	25
3.3.2	Peripheral interface controller (PIC).....	25
3.3.3	MOSFET.....	26
3.3.4	Capacitors.....	29
3.3.4.1	Bypass capacitors.....	29
3.3.4.2	Resonance capacitors.....	30
3.3.4.3	The smoothing capacitor.....	31
3.3.5	Voltage Regulator IC.....	31
3.3.6	Coils.....	32
3.4	Summary.....	35
CHAPTER FOUR		36
4. DESIGN AND IMPLEMENTATION OF WIRELESS POWER TRANSFER SYSTEM		36
4.1	Introduction.....	36
4.2	Theoretical Model Calculation.....	36
4.2.1	The Conditions of Resonance in RLC Circuit.....	36
4.2.2	Efficiency Formula.....	37
4.3	The Experimental Setup.....	39
CHAPTER FIVE		43
5. EXPERIMENTAL RESULTS AND DISCUSSION		43
5.1	Experimental Measurements Procedures.....	43
5.2	The Experimental Results of the Basic Circuit Design of WPT System.....	44
5.3	The Influence of Ferrite Materials.....	49
5.4	The Experimental Results of the Design With Using Ferrite of WPT System.....	51
5.5	Results Comparison with and without using Ferrite.....	55
5.5.1	Results Comparison of the Load Resistance Variation Test.....	55
5.5.2	Comparing the Transfer Efficiency over Distance.....	58
CHAPTER SIX		61
6. CONCLUSIONS AND FUTURE WORK		61
6.1	Conclusion.....	61
6.2	Future Work.....	62
REFERENCES		63
CIRRUCILUM VITAE		67

LIST OF TABLES

Table 1.1 : Main differences between WTP system technologies	4
Table 3.1 : Components used in the design	35
Table 5.1 : Load resistance variation test of the basic circuit design when $V_{in}=9V$ $D=25mm$ $R_{load} = 5-50\Omega$	45
Table 5.2 : Load resistance variation test of the basic circuit design when $V_{in}=15V$ $D=25mm$ $R_{load} = 5-50\Omega$	46
Table 5.3 : Load resistance variation test of the basic circuit design when $V_{in}=9V$ $D=65mm$ $R_{load} = 5-50\Omega$	47
Table 5.4 : Load resistance variation test of the basic circuit design when $V_{in}=15V$ $D=65mm$ $R_{load} = 5-50\Omega$	48
Table 5.5 : Load resistance variation test with using ferrite when $V_{in}=9V$ $D=25mm$ $R_{load} = 5-50\Omega$	51
Table 5.6 : Load resistance variation test with using ferrite when $V_{in}=15V$ $D=25mm$ $R_{load} = 5-50\Omega$	52
Table 5.7 : Load resistance variation test with using ferrite when $V_{in}=9V$ $D=65mm$ $R_{load} = 5-50\Omega$	53
Table 5.8 : Load resistance variation test with using ferrite when $V_{in}=15V$ $D=65mm$ $R_{load} = 5-50\Omega$	54
Table 5.9 : Comparing the efficiency over the distance with and without using Ferrite when $V_{in}=9V$ $D=10-380mm$ $R_{load} = 5\Omega$	59
Table 6.1 : Maximum efficiencies of the WPT system with and without using ferrite	62

LIST OF FIGURES

Figure 1.1	: Basic circuit diagram of wireless power transfer system.	2
Figure 2.1	: Principle of operation of an inductive power transfer system	11
Figure 2.2	: Basic block diagram of an inductive wireless power transfer system	12
Figure 2.3	: The magnetic flux (a) Magnetic flux produced by a current passing in a coil, and (b) The total magnetic flux produced due to i_1 crossing both coils	13
Figure 2.4	: Current distributions for the proximity effect with the current flow in the same direction.....	15
Figure 2.5	: Current distributions for the skin effect with the current carrying conductor.	16
Figure 2.6	: The equivalent series resistance of a conductor.....	16
Figure 2.7	: Magnetically coupled circuit	17
Figure 2.8	: Equivalent circuit of two magnetically coupled circuits	18
Figure 2.9	: Circuit diagram of resonant coupling with capacitors C1 and C2.....	18
Figure 3.1	: Block diagram of the wireless power transfer system	20
Figure 3.2	: Zener diode symbol model number 1N4733A	23
Figure 3.3	: Zener diode regulator circuit	23
Figure 3.4	: Schottky diode (a) Schottky diode symbol, and (b) Schottky diode model number SS36.....	24
Figure 3.5	: Diode Bridge Rectifier (a) The symbol model number W10M, and (b) Full wave bridge rectifier Circuit Diagram	24
Figure 3.6	: Infrared LED Light Emitting Diode symbol.....	25
Figure 3.7	: IC model number PIC12F683.....	25
Figure 3.8	: PIC12F683 IC connection diagram	26
Figure 3.9	: PIC output voltage signal.....	26
Figure 3.10	: N-Channel MOSFET (a) MOSFET symbol N-Channel, and (b) IRFZ44N MOSFET	27
Figure 3.11	: Operation of N-Channel MOSFET (a) when $V_{in} < V_{th}$ no current flow, and (b) when $V_{in} > V_{th}$ Current Flow.....	27
Figure 3.12	: Royer oscillator circuit schematic, first MOSFET is on. A positive square wave is produced through the transmitter coil.....	28
Figure 3.13	: Royer oscillator circuit schematic, second MOSFET is on. A negative square wave is produced through the transmitter coil.	28
Figure 3.14	: Signals from the transmitter and receiver coils (a) The transmitted signal, and (b) The received signal.....	29
Figure 3.15	: Purification of the noisy DC power source using bypass capacitors	30

Figure 3.16 : The output voltage of the rectifier is smoothed by adding a capacitor.....	31
Figure 3.17 : Voltage regulator IC (a) IC model number LM7805, and (b) IC pinout diagram	32
Figure 3.18 : Cross section of multi-layer, multi-row coil.....	33
Figure 3.19 : Multi-layer, multi-row copper coil (a) The transmitter coil, and (b) The receiver coil.....	34
Figure 4.1 : Equivalent circuit for theoretical model of WPT system	38
Figure 4.2 : Circuit diagram of transmitter circuit	39
Figure 4.3 : Circuit diagram of receiver circuit.....	39
Figure 4.4 : PCB layout design for transmitter circuit	40
Figure 4.5 : PCB layout design for the receiver circuit.....	41
Figure 4.6 : System hardware setup	42
Figure 5.1 : Measurement set-up in the laboratory	43
Figure 5.2 : Load resistance variation test of the basic circuit design when $V_{in}=9V$ $D=25mm$ $R_{load} =5-50\Omega$	45
Figure 5.3 : Load resistance variation test of the basic circuit design when $V_{in}=15V$ $D=25mm$ $R_{load} =5-50\Omega$	46
Figure 5.4 : Load resistance variation test of the basic circuit design when $V_{in}=9V$ $D=65mm$ $R_{load} =5-50\Omega$	47
Figure 5.5 : Load resistance variation test of the basic circuit design when $V_{in}=15V$ $D=65mm$ $R_{load} =5-50\Omega$	48
Figure 5.6 : Various shapes and sizes of ferrite cores.....	49
Figure 5.7 : Ferrite core during experimental tests	50
Figure 5.8 : Load Resistance Variation with using ferrite when $V_{in}=9V$ $D=25mm$ $R_{load} =5-50\Omega$	51
Figure 5.9 : Load resistance variation with using ferrite when $V_{in}=15V$ $D=25mm$ $R_{load} =5-50\Omega$	52
Figure 5.10 : Load resistance variation test with using ferrite when $V_{in}=9V$ $D=65mm$ $R_{load} =5-50\Omega$	53
Figure 5.11 : Load resistance variation test with using ferrite when $V_{in}=15V$ $D=65mm$ $R_{load} =5-50\Omega$	54
Figure 5.12 : Comparison of the load resistance variation test with and without using ferrite when $V_{in}=9V$ $D=25mm$ $R_{load} =5-50\Omega$	55
Figure 5.13 : Comparison of the load resistance variation test with and without using ferrite when $V_{in}=15V$ $D=25mm$ $R_{load} =5-50\Omega$	56
Figure 5.14 : Comparison of the load resistance variation test with and without ferrite when $V_{in} =9V$ $D = 65mm$ $R_{load} = 5-50 \Omega$	57
Figure 5.15 : Comparison of the load resistance variation test with and without using ferrite when $V_{in}=15V$ $D=65mm$ $R_{load} =5-50\Omega$	58
Figure 5.16 : Comparing the transfer efficiency over the distance with and without using ferrite when $V_{in}=9V$ $D=10-380mm$ $R_{load} =5\Omega$	59

LIST OF ABBREVIATIONS

WPT	:	Wireless Power Transfer
LF	:	Low Frequency
HF	:	High Frequency
RF	:	Radio Frequency
K	:	Coefficient of Coupling
Q	:	Quality Factor
PTE	:	Power Transfer Efficiency
M	:	Mutual Inductance
EMF	:	Electromotive Force
Φ	:	Magnetic Flux
r_L	:	Equivalent Resistance
Z_{ref}	:	Reflected Impedance
Z_L	:	Load Impedance
LED	:	Light Emitting Diode
PIC	:	Peripheral Interface Controller
f_0	:	Resonance Frequency
δ	:	Skin Depth
μ_0	:	Magnetic Permeability
ω_0	:	Angular Frequency
PCB	:	Printed Circuit Board

ABSTRACT

DESIGN AND IMPLEMENTATION OF AN ENHANCED WIRELESS POWER TRANSFER SYSTEM

AL-HASHEMI, Khalid

M.Sc., Department of Electrical Engineering

Supervisor: Prof. Dr. Doğan ÇALIKOĞLU

December 2017, 67 pages

Wireless power transfer (WPT) based on resonant inductive coupling of two coils are introduced. Literature survey of different types of WPT technology has been presented. Basic circuit of WPT system is designed and implemented. The proposed basic design has been enhanced by utilizing maximum possible magnetic field that is generated by the transmitter coil. Maximizing the effective magnetic field is achieved by using a ferrite core. The effects of the magnetic permeability of the ferrite core are investigated. The experimental tests are carried out with and without using ferrite core in the basic design. The operation frequency is about 30KHz, the two models have been measured in laboratory with different parameters and the results have been compared. As a result, optimum DC power supply and load resistance values have been measured and the effect of the ferrite has observed when the distance between transmitter and receiver coils is increased.

Keywords: Wireless power transfer, Ferrite core, Magnetic permeability, Power transfer efficiency.

ÖZET

GELİŞMİŞ KABLOSUZ GÜÇ TRANSFER SİSTEMİNİN TASARIMI VE UYGULANMASI

AL-HASHEMI, Khalid

Yüksek Lisans, Elektrik Mühendisliği Bölümü

Danışman: Prof. Dr. Doğan ÇALIKOĞLU

Aralık 2017, 67 sayfa

İki bobinin rezonant endüktif kuplajına dayanan kablosuz güç transferi (WPT) tanıtılmıştır. Çeşitli WPT teknolojilerinin literatür taraması sunulmuştur. WPT sisteminin temel devresi tasarlanmış ve uygulanmıştır. Önerilen temel tasarım, verici bobini tarafından üretilen maksimum olası manyetik alanı kullanarak artırılmış. Etkin manyetik alanı maksimize etmek ferrit çekirdeği kullanarak elde edilmiştir. Ferrit çekirdeğin manyetik geçirgenliğinin etkileri araştırılmıştır. Deney testleri ferrit çekirdeğini temel tasarımda kullanarak ve kullanmadan gerçekleştirilir. İşletim frekansı yaklaşık 30KHz olarak ayarlanmış, iki model laboratuarda farklı parametrelerle ölçülmüş ve sonuçlar karşılaştırılmıştır. Sonuç olarak, optimum DC güç kaynağı ve yük direnç değerleri ölçülmüş ve verici ve alıcı sargıları arasındaki mesafe arttıkça ferritin etkisi gözlemlenmiştir.

Anahtar Kelimeler: Kablosuz enerji transferi, ferrit çekirdek, manyetik permeabilite, güç transfer verimi.

CHAPTER ONE

1. INTRODUCTION

1.1 Presentation of the Work

The objectives of this project are to design and implement a system with the ability to transfer power from a source to a load without a physical connection and to make theoretical and practical investigations to obtain superior performance. This system must achieve the following

1. Obtaining high transferred power efficiency for the proposed design wirelessly.
2. Minimizing the numerous losses that occur due to the transfer of power due to reluctance of the magnetic circuit.
3. Linking the transmitter circuit with the receiver circuit with a high possible coupling coefficient.
4. Preventing the mismatches of the elements by a high level of compatibility between the components of the system.

1.2 Wireless Power Transfer

Wireless power transfer (WPT) is the transmission of electrical power from a power source to an electrical load without the use of cables. The main concept of a WPT system is to build two systems. The first system is the transmitter, which comprises the power source. The second system is the receiver, which comprises the load, these systems have to work harmoniously with each other.

The standard power source for movable devices is a battery. Most of these devices are powered by rechargeable batteries which need repeated recharging. Therefore, using wireless power transfer to charge batteries wirelessly is a typical

solution in cases where direct contact with a power source is risky, impossible, or expensive.

This technique faces many issues including cost, distance, losses of transferred power and the volume of the system even though scientists continue to provide us with inventions that make life easier and more comfortable.

Wireless power transfer systems consist of a transmitter device which is connected to a power source and one or more receiver devices that receive the transferred power. Transmission occurs via a number of coupling elements, see Figure. 1.1 [1]. These elements include the following:

1. A coil which produces a magnetic field.
2. A metal plate which produces an electric field.
3. An antenna which produces radio waves.
4. A laser which produces light.

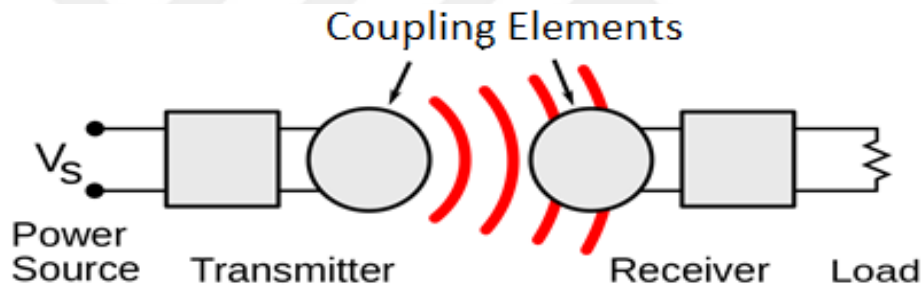


Figure 1.1: Basic circuit diagram of wireless power transfer system.

1.2.1 The Importance of WPT and Its Applications

In last couple decades, interest in studies and the improvement of wireless power transfer technology has been growing to dispense with the use of cables after wireless becomes broadly universal and accepted. If we were to imagine lying in bed and playing game in our cell phone, the phone would start to charge and there would be no cable plugged into the device, we could easily take our mobile device on our way out and charge it anywhere we went, whether at home, at school, in a restaurant and even in a public park. We might certainly forget to bring our chargers, USB cables and power adapters, etc., but day by day, the use of electronic devices has become more essential and indispensable in our lives as well as becoming increasingly involved in almost every aspect of our lifestyle.

Applications of WPT:

- 1- Charging mobile devices: Instead of having to have charging cables everywhere, one can simply put a mobile device onto a charging pad and it will automatically begin to charge, which may be appropriate in terms of easy and more comfortable usage for devices such as cell phones, laptop computers and cameras, or it may be appropriate in terms of avoiding electric shocks due wet environments such as when using an electric toothbrush.
- 2- Point-to-Point WPT: Providing electrical power might be costly or impossible on some special terrain such as islands or mountain peaks, hence, WPT may be the best alternative solution [2].
- 3- Charging electric vehicles: The new technology of electric trains or buses would start to operate on batteries, and it would help to prevent mechanical contact with the source of power and with what is caused by friction. However, such batteries need to be charged repeatedly. Therefore, we can involve WPT to charge vehicle batteries by using magnetic field when vehicles are parked or by using electromagnetic waves when vehicles are in motion [2].
- 4- Solar power satellite: The basic idea is to convert sunlight into power using a satellite placed above the atmosphere and sending that power to the Earth via microwaves [3]. Microwaves have a characteristic such that they are not absorbable by meteorological conditions [2].
- 5- Charging implantable medical devices: Devices that are implanted inside the body such as cochlear implants and pacemakers stay inside the body for a long time and need to have their batteries charged repeatedly. Since it is impossible to charge them via external charging ports, WPT is the obvious solution to avoid dangerous and expensive surgery to replace any batteries.

1.2.2 Types of WPT Systems and Their Properties

The coupling mechanisms of a WPT system can be divided into three types:

1. Inductive coupling in low frequency (LF) bands.
2. Resonant coupling in high frequency (HF) bands.
3. Radio frequency (RF) radiation [4].

Inductive coupling has a short range (a few centimetres) with high efficiency. Nowadays, commercial companies focus on using this type of technology for cordless cell phone chargers.

Resonant coupling has a longer range than inductive coupling (up to two meters) with high power. For instance, in mid-2007, researchers at the Massachusetts Institute of Technology succeeded in transferring 60 watts at a range of two meters at up to 40% efficiency by using a resonance frequency equal to 10.56 ± 0.3 MHz using strongly coupled magnetic resonance [5]. The main idea of this type of WPT is that both the transmitter and receiver with same resonance frequency can exchange power in good form, with even one meter being sufficiently good to charge mobile devices. The last type is RF radiation, which has long range (space applications) [6], which is why it transfers only a few milliwatts of power. Using RF radiation over long distances needs an antenna and is risky for human beings.

Table 1.1: Main differences between WTP system technologies [5]

	Induction coupling	Resonant coupling	Radiative Transfer
Wave	Magnetic field (Wideband)	Magnetic field (Narrow band)	Electromagnetic wave
Rang	Very short (cm)	Short (m)	Medium and Long (km)
Efficiency	High	Medium	Low
Operating Frequency	LF-band (several hundred kHz)	HF-band (6.78MHz-13.56MHz)	RF-band (2.4GHz-5.8GHz)
Typical load	Varying load (battery)	Fixed Impedance	Fixed Impedance
Advantage	High Efficiency	Medium efficiency in a short rang	Long rang
Bottleneck	Very short rang	Difficulties in maintaining high Q	Low efficiency, Human Safety

WPT refers to several different types of wireless power transmission technology. Selecting the appropriate type depends on the desired distance, efficiency, environment, cost, and so on.

In cases of using magnetic field, the signal at the end of a transmitter device (coil) should be alternating current (AC) because oscillating signal create dynamic magnetic fields and dynamic electric fields around the coil. Dynamic fields can carry

power in contrast to direct current (DC), which creates static fields and can carry only information.

In cases of using radiative transfer, the same signals and fields that are used in wireless communication devices (broadcasting, cellphones, WI-FI and radio) are being use in radiative transfer. However, in radio communication, the aim is to transfer information, and a small amount of power will transfer, therefore, the amount of delivered power in a receiver is insignificant, unlike a WPT, where the portion of transmitted power that is acquired by receiver is a very important parameter [7].

1.3 Literature Survey

Both induction coupling and resonant coupling use magnetic field (see Table 1.1). However, inductive WPT is likely the most in use these days because of its high efficiency and low frequency requirements. Resonant coupling strength depends on the strength of resonance phenomenon between the transmitter and the receiver circuits. It is controlled by tuning the capacitors, unlike induction coupling which work like transformers, where the strength of coupling depends on the strength of the flux linkage between the primary and secondary coils, which comprises the transmitter and receiver coils in WPT.

Kurs et al. (2007) [5] succeeded in transferring 60 watts to light a bulb at a range of two meters at up to 40% efficiency by using four coils, two of which were connected to the source and load and the other two inductively coupled to each other. the frequency used was $f = 10.56 \pm 0.3\text{MHz}$.

One year later, Justin R. (2008) [8], chief technology officer of Intel Corporation, used a magnetic field for a 60-watt lamp at a range of one meter at 75% efficiency. Two years after that, researchers from Intel Corporation (2010) [9], designed a WPT device, the receiver part of which did not require being placed in a straight line with transmitter part. It could move in free space at angles up to 70° and transfer power up to a range of 70 centimeters. A positive achievement of this was that the efficiency decreased by only 30%. This characteristic would be useful in cases of charging portable devices such as cell phones, digital cameras, laptops or mp3 players.

Here, researchers have faced a new challenge. Therefore, Karalis and Kurs (2010) [10] found that the resonance between the elements of a WPT system would increase the efficiency of the power transfer and the power loss rate would be

small compare to the power transfer rate. Furthermore, the transmitter could still in couple with the receiver even with varying distances between them, therefore, greater mobility occurs. They therefore proposed to put the transmitter in ceilings while devices roaming freely can charge in the room.

Kiani and Ghovanloo (2013) [11] designed three WPT systems with different power levels. The first system had two coils which were strongly coupled and high power was delivered to the load, which is needed in microelectronic devices. The second system had three coils, which was suitable and even when the distance between the transmitter and receiver varied, a large power delivered to the load was still achieved, such as what can be found in some cellular phone chargers. The third system had four coils. This system operated optimally when the distance between the transmitter and receiver was constant and power transfer efficiency (PTE) was significant, such as when being used to charge electric vehicles.

From the above studies, producing high power delivered to the load or PTE depends on maximizing the coupling between a transmitter's coil(s) and receiver's coil(s), which is a result of having multiple coils in the system.

RamRakhyani. and Lazzi (2013) [12] studied and experimented with using more than two coils to transfer power wirelessly. They found that this caused an increase in the quality factor (which is the ratio of inductive reactance to resistance at a certain frequency of the coils), and hence an improvement in the transfer efficiency.

Lee and Cho (2015) [13] studied the provision sufficient energy to each load coil in a multi-receiver system since the greater power tended to be delivered to the nearest load coil. This was done by adjusting the power between the receivers by using coupled mode theory.

Jiwariyavej and Imura (2015) [14] presented derivations of equations for estimating coupling coefficients (K).

However, having coupling coefficient values in WPT systems will help to improved charging efficiency and it will help in knowing how much power to distribute to a receiver (or to receivers in cases of multi-receivers). They studied the equations of coupling coefficients either from the source side (transmitter side) or load side (receiver side). They finally found that estimating the coupling coefficients from the load side can be done better than from the source side because more than one receiver may be involved. For instance, charging can occur for more than one electrical

vehicle or more than one cellphone with only one source.

Nair and Choi (2016) [15] found that the use of a system consisting of many loop coils of different sizes can solve the issue of movable transmitters and/or receivers. In other words, certain varying distances between the transmitter and receiver are available. However, this causes the coupling parameters to change, and as a result, the efficiency of the transferred power changes. Moreover, to keep the efficiency constant through this variation of distance, they proposed to use a multiple coil switching system that can redistribute the power harmony among these many coils by switching the power between them, which allowed them to calibrate the coupling coefficient (K) equally. However, K is the amount of available inductive coupling between the two coils with value between 0 and 1. Some researchers use more coils in order to maximize the efficiency of the transmitting power. For transferal of power over long distances, magnetic fields are not suitable, so electromagnetic waves are used instead, hence, a special type of antenna, known as a rectenna, is used in this type of transferal. This rectifying antenna functions to convert electromagnetic waves into direct current. The transmitting antenna converts the electrical current into electromagnetic waves and the receiving antenna (rectenna) converts these electromagnetic waves back into electrical current [16]. Here, the selection of a suitable frequency for the antennas in each application becomes important.

Poon and O'Driscoll (2007) [17] examined a WPT system by using an antenna with a sufficiently high frequency to minimize the effect on human tissues. They studied the possibility of minimizing the size of an antenna 10,000 times which would operate at a frequency of 1 GHz rather than at 10 MHz, but only over short distances.

Recently, WPT systems have solved the issue of charging batteries for implantable medical devices such as cochlear implants and wearable cardiac pacemakers. However, implanted devices inside the body require a continuous supply of power since it is impossible to connect these devices to an external source via cables. However, implanted devices inside the body operate by battery and all batteries have a limited life and need to be charged repeatedly, and WPT is the best way to do so. These systems have three parts: a transmitter system (which generates an alternating magnetic field), a transmitter and receiver coils, and the receiver system, which is implanted inside the body and works to receive an alternating magnetic field to be converted into direct current to charge the internal batteries. One major concern is to

prevent charging of a battery when it is full. Such issue can be avoided through the use of relay based switching circuits [18], Here, researchers face another challenge, which is to design a very small WPT system, especially the receiver part due their increasing use in the body as implanted devices. J. Lee and Sangwook (2010) [19] used two small antennas to transfer power wirelessly. They characterized the interaction between these small antennas by using an impedance parameter. Moreover, they studied the optimum load impedance and maximum efficiency of transferred power as functions of the distance between these small antennas.

Chen and Zhang (2015) [20] improved the WPT circuit which transfers both power and information. By using a multi-antenna, the challenge was the fact that transferring both power and information causes channel fading and signal attenuation, and as a result, it reduced the signal transmission distance. Another challenge was to find best way to obtain high efficiency in both the power and information simultaneously with the same parameters. Their last challenge was to secure the transferred data and its effect on the efficiency of the transferred power by exploiting the spatial degree of the multi-antenna.

1.4 Motivation

The increasing use of portable devices (cell phones, digital cameras, PDAs, laptop computers and mp3 players) and their new technology development causes us to find ways to use them with more mobility while they are charging. Disposing of charging cables is the best way to this. Charging them wirelessly is the new alternative technology which will also save on the wiring costs and avoid electrical shock hazards. Moreover, some applications acquire power through mechanical contact, such as electric trains, therefore, wireless power transfer is the best choice to deal with this matter.

As explained in the following chapters, many researchers focus on improving transferred power efficiency by resonant coupling and radio frequency, while our goal is to work on inductive resonance coupling in the low frequency (LF) bands to enhanced the power efficiency transferal, furthermore, to increase the distance of that transfer.

1.5 Main Aspect of the Work

In this project, a wireless power transfer system has been designed and implemented. The system consists of two parts: the transmitter circuit and receiver circuit, and it being divided into numerous blocks, starting from a source finishing at the load. Each block has a specific function and contains many elements. However, the system was studied step by step and the elements were tested for compatibility with each other to prevent any mismatching between them and to protect them from the hazard of damage. The values of frequency, capacitance and inductance were selected accurately to have the circuit subjected to resonance phenomena.

Then, a prototype has implemented and referred to as a basic circuit design. Many experimental tests were performed and the efficiency was calculated. For the next step, it was necessary to find a method to enhance the performance of the system by increasing the distance between the transmitter and receiver and by increasing the efficiency of the transferred power.

The amount of the magnetic flux that reaching a receiver coil determines the amount of the received power for a particular system, since this magnetic field is generated by the transmitter coil will scattering all around the place, as a result, the receiver coil catching only a small portion of it. Hence, it becomes necessary to direct and use more flux. Therefore, it is essential to increase the magnetic field thereby also increasing the mutual inductance. Materials with high magnetic permeability have the ability to form and direct the magnetic flux toward them. A soft ferrite core was chosen to do this due to its high magnetic permeability when placed in a magnetic field. In a laboratory, the same experimental tests that are performed with a basic circuit design have been repeated, but this time using the ferrite core by putting it behind the receiver coil. Mutual inductance and efficiency are calculated again, and comparisons between the two set of results (with and without using the ferrite core) are made. Finally, the results are discussed, and future work is presented.

1.6 Thesis Layout

This thesis consists six chapters, each of which deals with the following:

Chapter 1:

Presentation of the work, definition of wireless power transfer, literature survey, and the main aspect of the work.

Chapter 2:

Theoretical overview of wireless power transfer, mutual inductance, the equivalent circuit, and the principle of resonant inductive coupling.

Chapter 3:

Block diagram of a wireless power transfer system, and the components used in practical model design.

Chapter 4:

Theoretical model calculations and the experimental setup.

Chapter 5:

Laboratory measurements and experimental results.

Chapter 6:

Conclusion and future work.

References:

List of academic references.

CHAPTER TWO

THEORETICAL GROUNDS FOR WIRELESS POWER TRANSFER

2.1 Overview of an Inductive Power Transfer System

The two laws defining the principle of wireless power transfer magnetic induction are Ampere's Circuital Law and Faraday's Law. Ampere's Circuital Law states that when an electric current pass through a conductor, it causes production of a magnetic field around it, while Faraday's Law of Induction states that when a conductor is placed in a varying magnetic field, it causes an electromotive force (EMF) in it. Figure 2.1 shows how power is transferred through the air from the transmitter to the receiver according the principle of Ampere's Circuital Law and Faraday's Law.

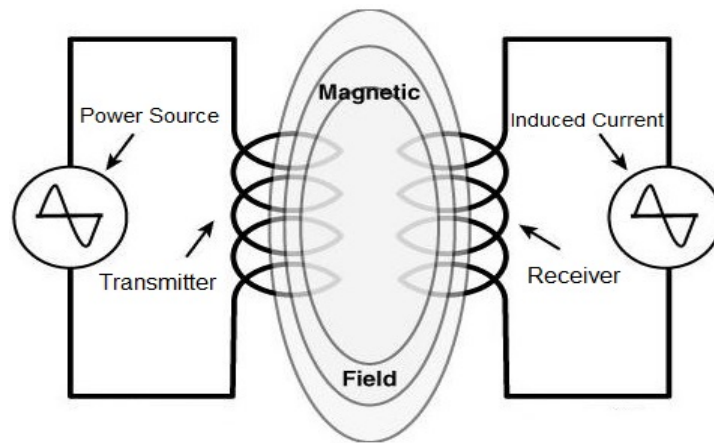


Figure 2.1: Principle of operation of an inductive power transfer system

However, passing an oscillating current through the first coil, which is presented as the transmitter, produces an oscillating magnetic field. On the other hand, if another coil, presented as the receiver, is sufficiently nearby, then an electromotive force in the second coil is produced because of that oscillating magnetic field as well as the any current passing into the load. In brief, this is the principle of wireless power transfer.

However, to have these two coils operate in a coupled manner and subjected to the mentioned laws, it is not necessary for them to have the same form and dimensions. Figure 2.2 shows the other stages that must be applied during the power transfer process. At the beginning, a voltage supply provides a direct power (DC), the next stage is DC/AC inverts to converts the DC voltage into AC voltage. Passing an oscillating signal through the coil produces an oscillating magnetic field. If this occurs and a nearby coil is exist with the assistance of an inductive link, an oscillating current is produced in the second coil. In most cases, a DC voltage is desired as we are charging batteries, therefore, an AC/DC converter may be used in such cases.

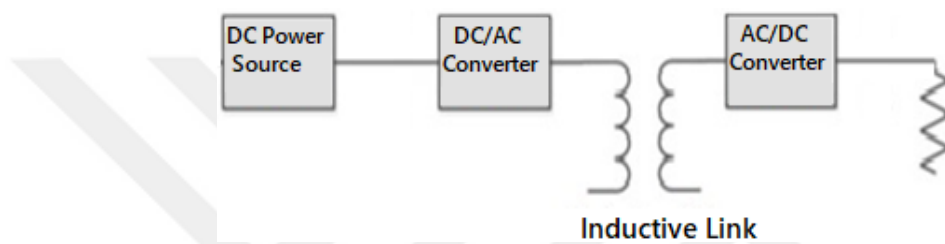


Figure 2.2: Basic block diagram of an inductive wireless power transfer system

2.2 Mutual Inductance Concepts and Coupling Coefficient

Magnetic coupling occurs between two coils if they are under conditions that allow them to be paired, or simply, it can occur when the magnetic field of one coil intersects with the field of the other coil. Here, self-inductances are produced in each coil in addition to another inductance produced between these coils known as mutual inductance (M).

Ampere's Law states that a when current i passes through a coil that produces a magnetic flux Φ , see Figure 2.3 (a), the magnetic flux is given by:

$$\Phi = \frac{\mu_0 N A}{w} \quad (2.1)$$

where:

μ_0 = the permeability of free space

A = the area of the coil

N = number of coil turns

w = the width of the coil

Faraday's Law of Induction states that a voltage is induced in a coil and it is proportional to the number of turns N and variation of the magnetic flux Φ over time, thus:

$$v = N \frac{d\Phi}{dt} \quad (2.2)$$

$$v = L \frac{di}{dt} = \frac{\mu_0 N^2 A}{w} \frac{di}{dt} \quad (2.3)$$

The self-inductance (L) of the coil is given by:

$$L = \frac{\mu_0 N^2 A}{w} \quad (2.4)$$

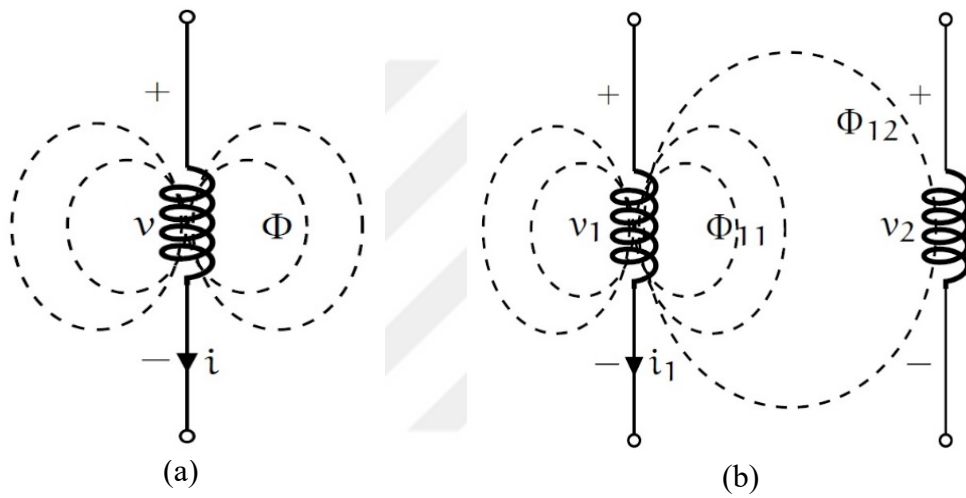


Figure 2.3: The magnetic flux (a) Magnetic flux produced by a current passing in a coil, and (b) The total magnetic flux produced due to i_1 crossing both coils

When two coils are paired, then the overall flux Φ_1 produced by the primary coil has two components, flux Φ_{11} which surrounds the primary coil and Φ_{12} which surrounds the secondary coil, see Figure 2.3 (b). The overall flux produced by the primary coil is given by:

$$\Phi_1 = \Phi_{11} + \Phi_{12} \quad (2.5)$$

Then, the voltage induced in primary coil given by:

$$v_1 = N_1 \frac{d\Phi_{11}}{dt} \quad (2.6)$$

While, the voltage induced in secondary coil given by:

$$v_2 = N_2 \frac{d\Phi_{12}}{dt} \quad (2.7)$$

Equations 2.6 and 2.7 can be written respectively as:

$$v_1 = N_1 \frac{d\Phi_1}{di_1} \frac{di_1}{dt} = L_1 \frac{di_1}{dt} \quad (2.8)$$

$$v_2 = N_2 \frac{d\Phi_{12}}{di_1} \frac{di_1}{dt} = M_{21} \frac{di_1}{dt} \quad (2.9)$$

L_1 is the self-inductance of the primary coil and M_{21} is the mutual inductance of the secondary coil with respect to the primary coil. M_{21} is given by:

$$M_{21} = N_2 \frac{d\Phi_{12}}{di_1} \quad (2.10)$$

In cases of passing current i_2 through the secondary coil, the overall flux produced by the secondary coil is given by:

$$\Phi_2 = \Phi_{22} + \Phi_{21} \quad (2.11)$$

Moreover, by applying the same equations above, we can calculate the voltages v_1 induced in the primary coil, the voltages v_2 induced in the secondary coil and the mutual inductance M_{12} of the primary coil with respect to the secondary coil. In summary:

$$M_{21} = M_{12} = M \quad (2.12)$$

This brings to light the mutual inductances M_{12} and M_{21} having the same value when applying a voltage source on either side with the specifications of the same coils [21]. M is referred to as the mutual inductance between the two paired coils, and is measured in henrys (H) such as self-inductance. However, calculating mutual inductance can be carried out experimentally by using the no-load method, which means the receiver circuit is an open circuit, and by applying the following equation [22] [23]:

$$M = \frac{V_2}{2 \pi f I_1} \quad (2.13)$$

where V_2 is an induced voltage in the receiver coil when the receiver circuit is open, f is the operation frequency and I_1 is a current passing through the transmitter coil when the receiver circuit is open.

The ratio of the mutual inductance to the self-inductance measures the strength of coupling between the two paired coils. Here, an important factor appears and affects WPT performance, which is the coupling coefficient (K). It defines the amount of available inductive coupling between the two paired coils and is given by:

$$K = \frac{M}{\sqrt{L_1 L_2}} \quad (2.14)$$

It has a value between 0 and 1, so when $K = 0$, no inductive coupling is available. When $0 < K \leq 0.5$, the two coils are loosely coupled. When $0.5 < K < 1$, the two coils are in tightly coupled. When $K = 1$, full inductive coupling occurs.

2.3 Equivalent Series Resistance of the Coils and Quality Factor

Inductors are often supposed to be pure inductors. In fact, they have a finite quantity of resistance, therefore, these inductors are series resistance and the current through the coils turns into heat, thereby causing a loss of inductive quality. Many resistances appear in coils when they drive an oscillating current rather than direct current. The proximity effect and skin effect are two of these effects. However, the proximity effect occurs when two or more adjacent conductors are carrying an oscillating current, in case of coil, the current flow in the conductors with the same direction. The magnetic fields that produced from them interact and repel each other in the regions where they approach each other and cause the current not to pass in this region, see Figure 2.4. The skin effect occurs when oscillating current passes through a conductor and the surface of that conductor carries more current compared to its centre because the surface has a lower counter electromotive force than the centre due to a higher magnetic flux produced in it, see Figure 2.5.

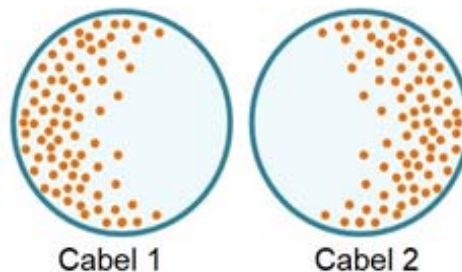


Figure 2.4: Current distributions for the proximity effect with the current flow in the same direction.

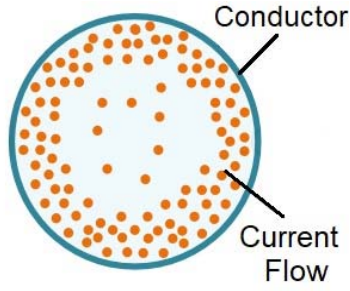


Figure 2.5: Current distributions for the skin effect with the current carrying conductor.

However, the proximity effect and skin effect change proportional to the frequency [24]. Thus, the equivalent resistance r_L of a conductor at a given frequency can be written as:

$$r_L = r_{DC} + r_{Proximity} + r_{Skin} \quad (2.15)$$

When r_{DC} is the resistance at zero frequency (DC), $r_{Proximity}$ is the resistance that is generated by the proximity effect and r_{Skin} is the resistance that is generated by the skin effect.

In summary, r_L represents the equivalent series resistance of a conductor that is driven by a particular frequency, see Figure 2.6.

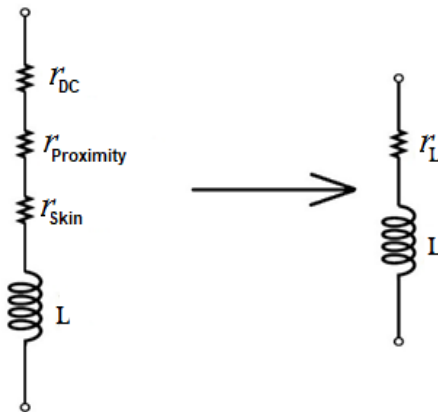


Figure 2.6: The equivalent series resistance of a conductor

Hence, the ratio between the inductive reactance to the resistance of a conductor at a certain frequency is known as the quality factor (or Q), given as:

$$Q = \frac{\omega L}{r_L} = \frac{X_L}{r_L} \quad (2.16)$$

where $\omega = 2\pi f$

2.4 The Equivalent Circuit

Circuits with coupled coils can be resolved by obtaining the values of the currents and voltages and other parameters. However, before doing so, it is necessary to find the equivalent circuit to eliminate any complex calculations due to any additional parameters that occur during the coupling. Figure 2.7 shows two coupled circuits. Symbols of the parameters of the first circuit (which are connected to the source) follow with the number '1' and the parameters of the second circuit follow with the number '2'. However, this equivalent circuit helps to determine the voltage across the first coil v_{L1} , the current passing through first coil i_1 , the induced voltage v_{L2} , the induced current in the second coil i_2 and the power dissipated in R_2 .

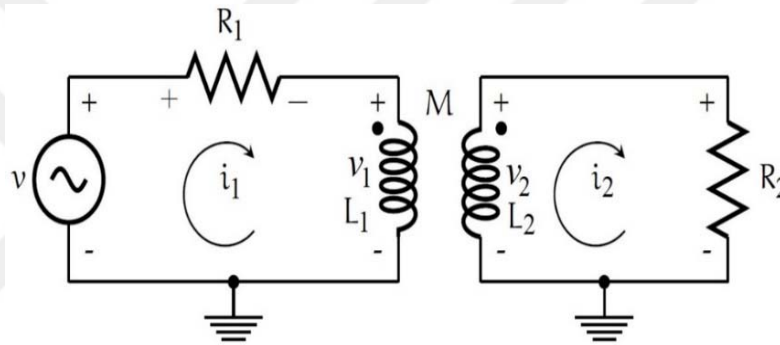


Figure 2.7: Magnetically coupled circuit

Circuits that contain only the main components connected in series, such as resistors and inductors, make calculations as simple as possible. Figure 2.8 shows the new simple design of a circuit coupled magnetically. The components of the second circuit are analyzed and reduced to the reflected impedance Z_{ref} , which is a combination of the components of the second circuit with the mutual impedance, given by:

$$Z_{Ref} = \frac{X_M^2}{r_{L2} + jX_{L2} + Z_L} \quad (2.17)$$

where X_M is the mutual inductance from Equations (2.10) and (2.12), r_{L2} is the equivalent series resistance of the first coil from Equation (2.15), jX_{L2} is the reactance of the second coil, and Z_L is the load impedance.

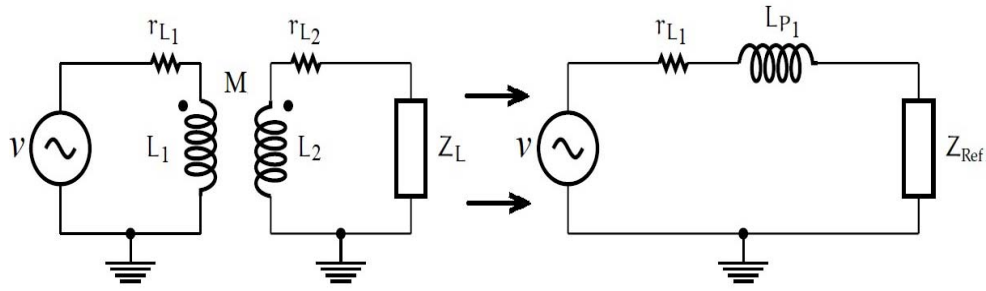


Figure 2.8: Equivalent circuit of two magnetically coupled circuits

2.5 Resonant Inductive Coupling

A resonant inductive coupling of a wireless power transfer system is similar to a basic resonant circuit that contains resistor(s), inductor(s) and capacitor(s). According to Equation (2.17), decreasing the reactance of the second circuit's coil X_{L2} causes an increase in Z_{Ref} and hence increase in the power transfer efficiency. However, to eliminate or at least to decrease any reactance in a particular circuit, we must add a capacitor that makes the circuit at the highest possible resistive load, which is the principle of resonance. In WPT systems, this can be achieved by, adding a capacitor to the circuit in both of transmitter and receiver circuit to makes it has a resistive load and hence increasing the power transfer efficiency due to increasing the reflected impedance [25], see Figure 2.9. Here, in an ideal resonance the Equation (2.17) will be:

$$Z_{Ref} = \frac{X_M^2}{r_{L2} + Z_L} \quad (2.18)$$

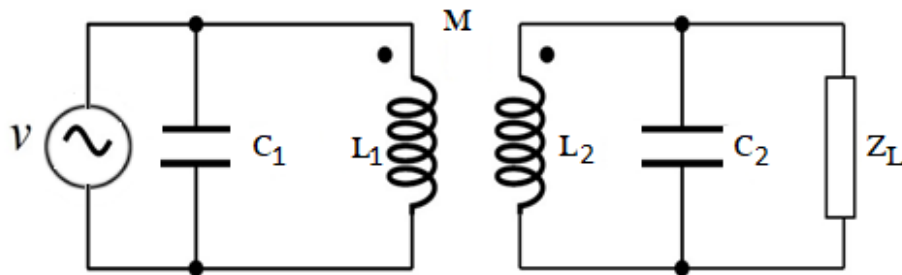


Figure 2.9: Circuit diagram of resonant coupling with capacitors C1 and C2

CHAPTER THREE

BLOCK DIAGRAM REPRESENTATION OF THE WPT SYSTEM AND ITS COMPONENTS

3.1 Introduction

Wireless power transfer systems based on magnetic inductive consist of several blocks. Modeling methodology required guidelines to select an efficient and effective system. Making the parameters of each block work as idealistically as possible, it is necessary to find matches between their parameters. This is the principle of the resonance phenomenon. In this chapter, phases of the block diagram will be explained individually and separately. The blocks containing various elements used in our design will also be describe.

3.2 Block Diagram of the Wireless Power Transfer System

Initially, a DC source provides power to the system, regulated the input voltage has a beneficial effect on the performance of the system. In the next phase is DC/AC converter, which converts direct current into alternating current. A varying magnetic field with time produces by alternating current that passes through the transmitter coil and wirelessly an electric field could be generated in the receiver coil if it interacts this field. Since most WPT applications charge batteries, an AC/DC converter has to be utilized. The final step is to use a regulated voltage in order to obtain precise direct voltage through the load, see Figure 3.1.

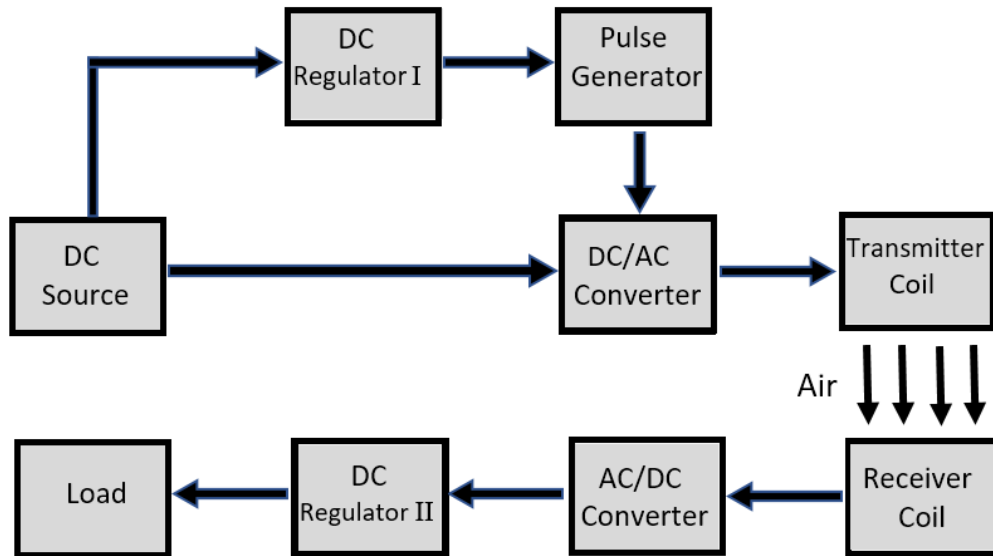


Figure 3.1: Block diagram of the wireless power transfer system

3.2.1 DC Power Supply Source

Power supply sources are devices that supply electrical power to an electrical load through an electric circuit. Unidirectional flows of electrical charge are referred to as direct current (DC), the sources of which can include power supplies, dynamos, batteries and solar cells. A power supply source usually provides a certain value to the load, which might be the current or voltage. In our project, 9-volt and 15-volt DC power sources were used.

3.2.2 DC Regulator I

The transmitter circuit of the WPT system needs to generate an oscillator signal. Therefore, an internal oscillator chip must be utilized for the task. This internal clock operates according to specific input values of voltage, current and power, for ensure it works properly, it is necessary to fixed those specific values by using regulator circuit. The Zener diode is being used in this project. The Roman numeral ‘I’ refers to the regulator circuit in the transmitter part as there is also another one in the receiver part, as explained later in this chapter.

3.2.3 Pulse Generator

As explained in the previous section, internal clock oscillator is used to generate high frequency pulses to feed transmitter circuit with the desired frequency which operates the system. In this project, a flash microcontroller IC was used.

3.2.4 DC/AC Converter

Producing an AC from a DC requires the use of an inverter which is fed by electrical pulses that are oscillator generated and will determine the frequency of the output signal. There are many different types of inverter that produce outputs with different waveforms, including square waveforms, sinusoidal waveforms and triangle waveforms. However, an inverter circuit needs a steady supply of voltage. Here, a square waveform is being used which is quite sufficient to generate an oscillating magnetic field to have the entire system operate optimally.

3.2.5 Transmitter Coil

The transmitter coil is the final terminal of the traveling signal. It could be a coil in the case of using the magnetic field technique to transfer the power, or an antenna in the case of using the electromagnetic wave technique. In our project, a circular coil of copper wire is used.

3.2.6 Receiver Coil

Choosing the parameters of a receiver coil is important since it determines the amount of mutual inductance that occurs between the transmitter and receiver coils, and thus we control the amount of transferred power efficiency. The coil contains inductance which helps the circuit reach its natural frequency, thereby making the circuit operate in resonance. In our project, a circular coil of copper wire is used.

3.2.7 AC/DC Converter

Batteries are the most common main power source of portable electric devices. They need a continuous DC power source in order to be charged, therefore, it is

necessary to convert the oscillating current that passes through the receiver coil into the direct current, hence the involvement of an AC/DC rectifier. The principle of the rectifier is to have the current flow in one direction in order to maintain a constant voltage level. In this project, a diode bridge rectifier was used.

3.2.8 DC Regulator II

Most portable electric devices charge their batteries at a standardized 5-volt DC voltage value. Thus, a voltage regulator must be used. A DC regulator controls a fixed output voltage that remains constant for any change in load. However, regulating the output voltage is optional in the receiver circuit. In our project, a voltage regulator IC was used.

3.2.9 The Load

Normally, power is transferred wirelessly to charge a battery which has specific load characteristics that need to be taken into account for the design and operation of the WPT system.

3.3 The Components

Different components are used during the implementation of the WPT model, including a DC power source, resistors, capacitors, different types of diodes, MOSFETs, copper wire, PIC microcontroller and a voltage regulator.

3.3.1 Diodes

In our design we have used eight diodes for four different functions, as following:

- 1- Zener Diode in parallel with the DC source.
- 2- Schottky Diodes which connected to the drain gate of the MOSFETs
- 3- Diode Bridge Rectifier across the receiver coil.
- 4- Light Emitting Diode across the receiver coil.

3.3.1.1 Zener diode

A Zener diode is a special type of diode which allows current to flow in the forward direction similarly to a regular diode, however, it also allows current to flow in the reverse direction when the voltage is above a limited voltage value, which is referred to as the breakdown voltage. Every Zener diode has its own breakdown voltage value, however, when a voltage is applied across the Zener diode in reverse bias and if this voltage is less than the breakdown voltage value, then the Zener diode becomes an open circuit. If the applied voltage is more than the breakdown voltage value, then the Zener diode acts to regulate the voltage according to its breakdown value. Zener diodes have many uses, especially to protect the components of the circuit when the value of the voltage should not exceed a specific value that might damage the circuit. Here, the resistor R_s is referred to as a current limited resistor which works to drop the remaining unregulated voltage, see Figures 3.2 and 3.3. In our design, a 5.1-volt 1N4733A Zener diode was used. When a voltage applied across the Zener diode in reverse bias is more than 5.1 V, the voltage will be regulated to 5.1 V. This will help to protect the other components of the circuit, especially the microcontroller IC.



Figure 3.2: Zener diode symbol model number 1N4733A

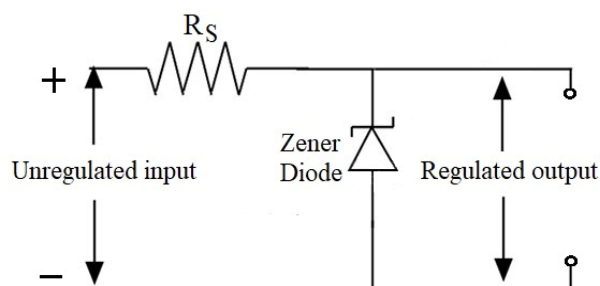


Figure 3.3: Zener diode regulator circuit

3.3.1.2 Schottky diode

It is another type of diode with a special characteristic dealing with a very high frequency signal because it has a very fast switching action and low forward voltage drops. In our design, we used two in the receiver circuit to protect the MOSFETs for the back EMF. The Schottky diode in our proposed design was the SS36 model, see Figure 3.4.

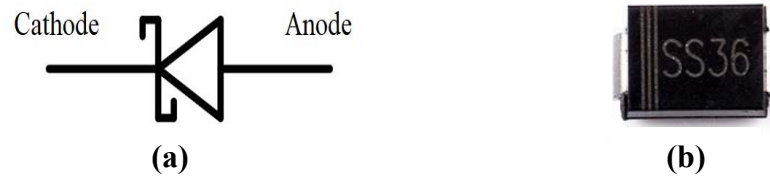


Figure 3.4: Schottky diode (a) Schottky diode symbol, and (b) Schottky diode model number SS36

3.3.1.3 Diode bridge rectifier

A diode bridge rectifier is an arrangement of four diodes, where the polarity of its output signal is same for either polarity of the input, as a result the output signal will be in a single direction, and the negative wave part will change its polarity and it will be eliminated, see Figure 3.5 (b). This is referred to as a rectifier, which converts AC to DC with the aid of a capacitor (or capacitors), which will be explained later in this chapter. However, another benefit of using a diode bridge is to prevent damage in circuits when the polarity of the source is installed unintentionally oppositely. In our design, a W10M diode bridge was used to convert the receiving power from AC to DC.

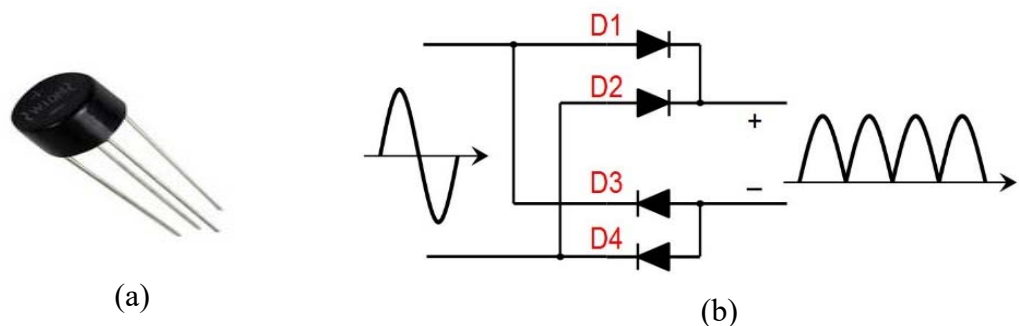


Figure 3.5: Diode Bridge Rectifier (a) The symbol model number W10M, and (b) Full wave bridge rectifier Circuit Diagram

3.3.1.4 Light emitting diode (LED)

An LED is a semiconductor device that acts as a diode. When the LED is forward biased (switched on), electric current passes through it and emits light, see Figure 3.6. In our design, infrared LED were used in a receiver circuit to indicate that the signal has been received.

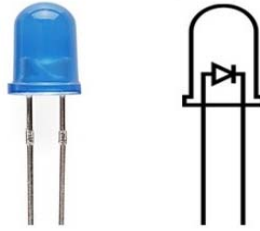


Figure 3.6: Infrared LED Light Emitting Diode symbol

3.3.2 Peripheral interface controller (PIC)

A PIC is a programmable integrated circuit that is used to generate pulses at a desired frequency to operate an inverter bridge circuit. The frequency of the pulses can be varied depending on the software with which the PIC is programmed. In this project, a PIC12F683 IC is used to generate square pulses that feed the gate terminal of the MOSFETs and turn them on and off sequentially, see Figure. 3.7. The PIC is fed by pin no.1 and its input operating voltage ranges between 2V and 5.5V, therefore, we used Zener diode to regulate the input voltage taken from a DC source from either 9V or 15V to 5.1V. A PIC is used in the design to enhance both of the performance of the switching and the output amplitude stability of the generated pulses. From the circuit connection shown in Figure 3.8, two square pulses will be generating from pins no. 2 and 3 to feed the gate terminal of the MOSFETs.



Figure 3.7: IC model number PIC12F683

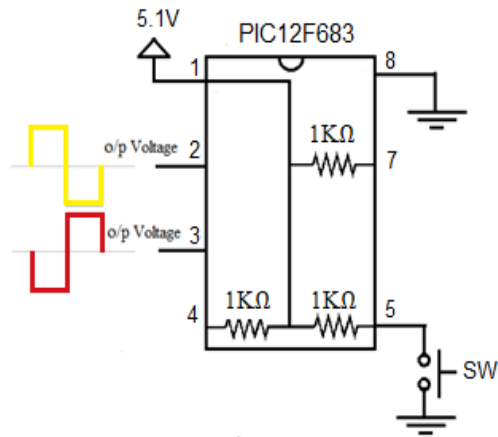


Figure 3.8: PIC12F683 IC connection diagram

The PIC is programmed using Proteus Design Suite professional software (version 7.10). Figure 3.9 shows the square pulses generated by the PIC. Channel A is the output from pin 2 and channel B is the output from pin 3.

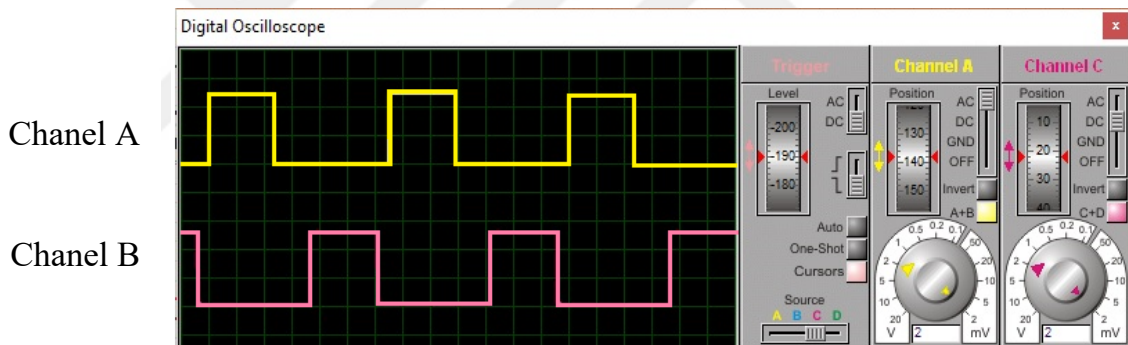


Figure 3.9: PIC output voltage signal

3.3.3 MOSFET

The MOSFET is a switching transistor that is used widely to amplify electronic signals in an electronic circuit. It has three terminals: drain (D), gate (G) and source (S), see Figure 3.10. The main advantage of using a MOSFET over other power semiconductor devices is the high-speed switching with picosecond precision.

However, a MOSFET needs pulses to turn it on and off, therefore, a pulse generator is used and feed the gate terminal. A MOSFET works as a switching device that will generate alternating current, which meets with requirement of producing an oscillating magnetic field to transfer power wirelessly.

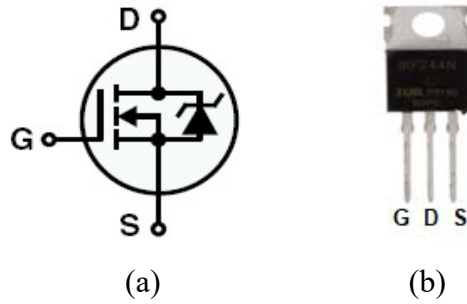


Figure 3.10: N-Channel MOSFET (a) MOSFET symbol N-Channel, and (b) IRFZ44N MOSFET

In our design, a basic Royer oscillator circuit was used consisting of two MOSFETs. The drain terminal of each MOSFET is connected with one terminal of the transmitter coil. The input power provides a DC current to the middle point of the transmitter coil. As a result, the transmitter coil has a center tap. When the input power source is applied, a direct current passes through the two coils until reaching the drain terminal of the two MOSFETs. Simultaneously, the pulses that the PIC generates appear in both their gate terminals and start to make the MOSFETs turn on and off sequentially. In other words, only one MOSFET turns on while the other turns off, and vice versa. A MOSFET operates when a voltage being applied to the gate terminal is larger than the threshold voltage (V_{th}), the MOSFET will turn on and the current passes through the channel between the drain (D) and source (S) and no current will pass through the gate into the MOSFET, see Figure 3.11.

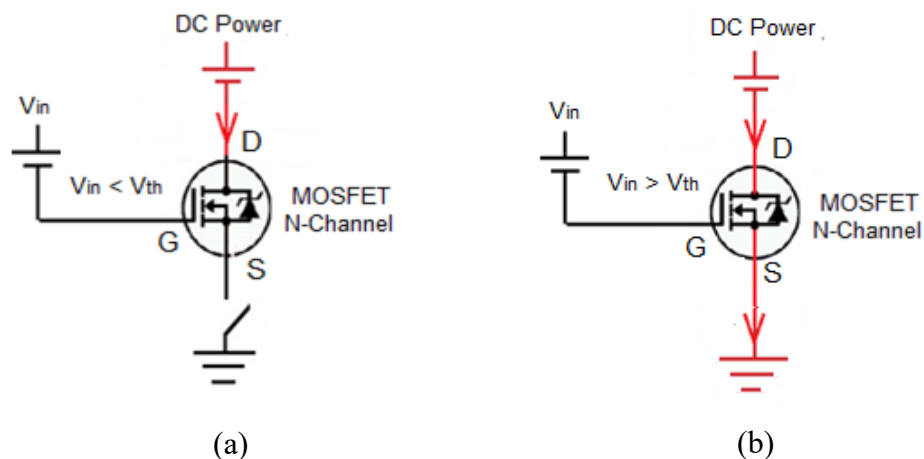


Figure 3.11: Operation of N-Channel MOSFET (a) when $V_{in} < V_{th}$ no current flow, and (b) when $V_{in} > V_{th}$ Current Flow

However, in the basic Royer oscillator circuit, the terminal (S) of both MOSFETs is grounded, thus, when the first MOSFET is on, depending on the pulse generated, the current at the (D) will flow to ground via (S), making the current flows through the half of the transmitter coil, while the other MOSFET is off and no current flows from (D) to (S), moreover, no current will flow through the second half of the coil. Then, the roles of MOSFETs will be reversed according the pulses that the PIC provide, and as a result, continuously feeding pulses to the gates of the MOSFETs causes the current to flow in the coil alternately, as a result, an alternating square wave will be generated, see Figures 3.12 and 3.13. In our design, two IRFZ44N MOSFETs were used and connected in a half bridge circuit.

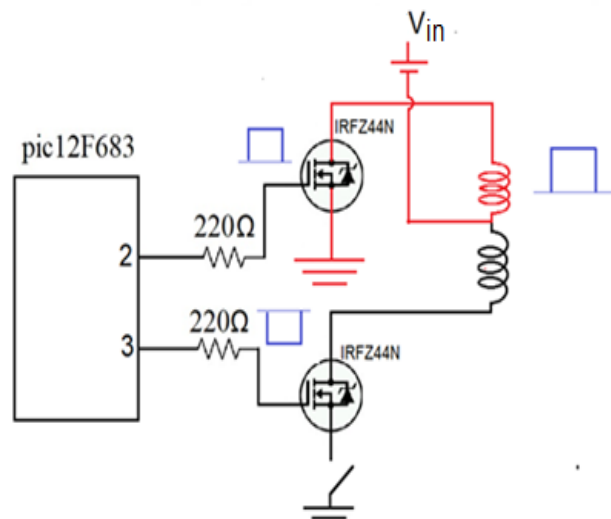


Figure 3.12: Royer oscillator circuit schematic, first MOSFET is on. A positive square wave is produced through the transmitter coil

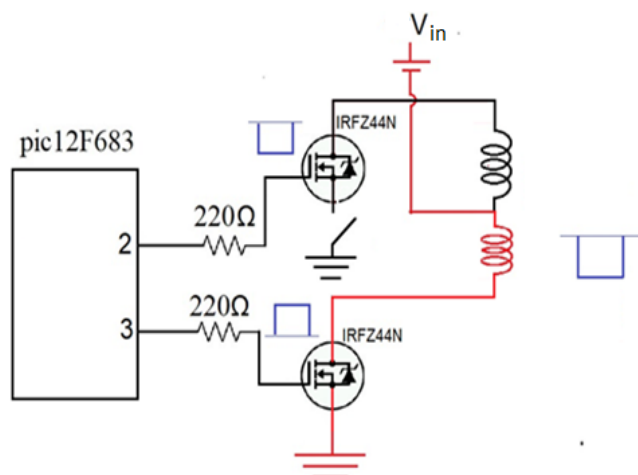


Figure 3.13: Royer oscillator circuit schematic, second MOSFET is on. A negative square wave is produced through the transmitter coil.



Figure 3.14: Signals from the transmitter and receiver coils (a) The transmitted signal, and (b) The received signal

3.3.4 Capacitors

In our design we have used seven capacitors for three different functions, as following:

- 1- Bypass capacitors in parallel with the DC source.
- 2- Resonance capacitors across the transmitter and receiver coils.
- 3- The smoothing capacitor across the output of the full wave rectifier circuit in the transmitter circuit.

3.3.4.1 Bypass capacitors

The bypass capacitors are used to filter out the ripple and noise over the DC voltage of the power source. These capacitors are used when pure DC input voltage is needed because high frequency noise might affect the performance of the circuit, especially when the circuit contains logic components such as ICs. As seen in figure 3.15. C1 is a $100\mu\text{F}$ aluminum polarized electrolytic capacitor uses to filter low frequency, as it is well-known electrolytic capacitors are not effective in filtering high frequency noise because of the inductance inherent in their construction. For this reason, it is necessary to use C2 which is a 100nf ceramic capacitor with a negligible inductance.

Bypass capacitors circuit were used twice in design, once with the DC power source in the transmitter circuit to feed the PIC with pure DC signal, and once with the rectifier circuit in the receiver circuit to obtain a pure DC output voltage.

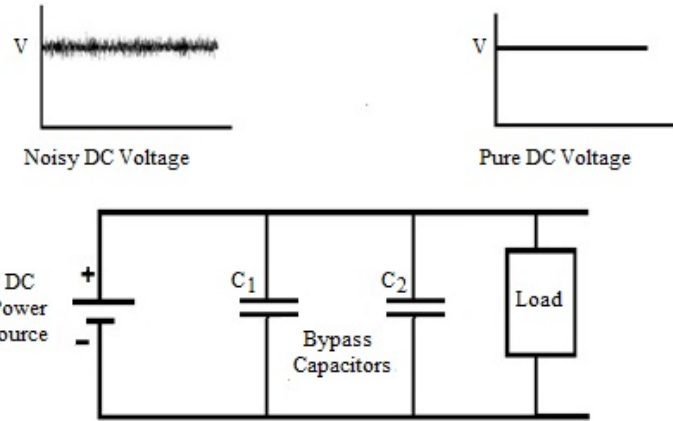


Figure 3.15: Purification of the noisy DC power source using bypass capacitors

3.3.4.2 Resonance capacitors

Resonant inductive coupling is a strong magnetic coupling between the transmitter and the receiver circuit. Each of these circuits contains inductance which is produced by the coils, and capacitance which is produced by the capacitors. In the RLC circuit, resonance occurs when the value of the inductive reactance X_L is equal to the value of the capacitive reactance X_C . Our design used parallel resonance. The impedance Z was then set at the maximum value. The signal received by radio is one of a number of significant resonance applications, but at a specific frequency. When the power transfer efficiency and mutual inductance are at their maximum possible values, it indicates the occurrence of a resonance phenomenon and this frequency is referred to as the resonance frequency (f_0). Adding a capacitor across the coil makes the circuit reach resonance. This capacitor also works to pass the AC component signal and prevent the DC component. In our project, the resonance capacitors were added in parallel across the transmitter and receiver coils.

The value of the capacitance was calculated using the given equation [26]:

$$f_0 = \frac{1}{2\pi\sqrt{LC}} \quad (3.1)$$

where f_0 = resonance frequency.

In our design the operation frequency is 30.6 kHz and both inductances of transmitter and receiver coil are 565 μH (which will be explained later in this chapter). Hence, the capacitance value (C) is $47.92 \times 10^{-9} \text{ F}$, so we add a 47 nano-farad capacitor to both of the transmitter and receiver coils.

3.3.4.3 The smoothing capacitor

As explained earlier in this chapter, a rectifier circuit is used to convert the receiving AC voltage into a DC voltage. A full wave rectifier bridge circuit converts the negative polarities of the input waveform into positive polarities. A sinusoidal waveform with only the positive wave part is not practical to use, so a suitable capacitor is added in parallel across the output of the full wave rectifier circuit, known as a smoothing capacitor. Such a capacitor converts the rippled waveform into a smooth DC waveform and produces a purer output DC signal similarly to a bypass capacitors, but the difference is that the bypass capacitor decouples the high frequency noise that generated by the power source, see Figure 3.16. In our design, we used a 100 μF capacitor.

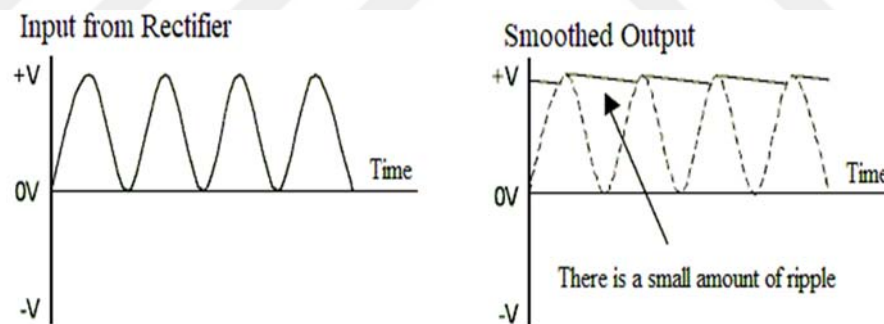


Figure 3.16: The output voltage of the rectifier is smoothed by adding a capacitor.

3.3.5 Voltage Regulator IC

A voltage regulator integrated circuit is used to maintain the amount of voltage at a fixed level. This regulator is an optional part in the receiver circuit. In our project, the LM7805 IC was used, see Figure 3.17. The two number 05s indicate the fixed output voltages it provides. We were choosing to regulate the output at 5V because most electrical devices charge their batteries at 5V.

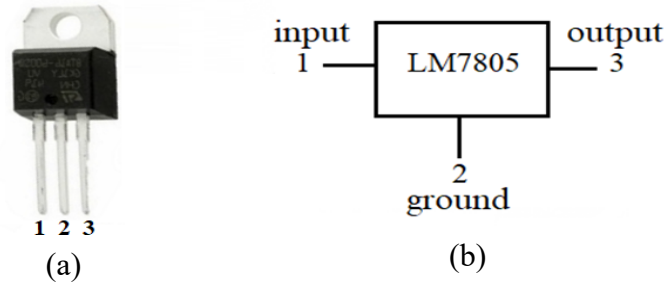


Figure 3.17: Voltage regulator IC (a) IC model number LM7805, and (b) IC pinout diagram

3.3.6 Coils

A coil is a loop (or loops) of a conductor wound to create an inductor. Many parameters determine the amount of inductance, such as the number of turns, coil size and the dimensions of adjacent conductors. In this proposed design, both the transmitting and receiving coils are symmetric, where 0.45 mm diameter copper wire was used. Coil diameter is 7.5 cm with 60 turns (the transmitter coil has a centre tap). A device with these specifications can handle a high current passing through it and the coils may become heated, especially the transmitter coil. In our design, the AC current of the transmitter coil is up to 1.3A.

However, the coils constitute the inductance and the parameters of the coils and capacitors connected across from them are selected to produce resonance at a particular frequency. The inductances of multi-layer, multi-row, cylindrical and air-core coils can be approximated calculated with the simple equation [27]:

$$L = \frac{0.8 a^2 n^2}{6a+9b+10c} \quad \text{microhenries} \quad (3.2)$$

where:

a = coil radius (center of coil to center of windings)

n = number of turns

b = coil length (distance from first to last winding)

c = winding depth.

All the dimensions are in inches and the parameters (a , b , and c) are indicated in Figure 3.18.

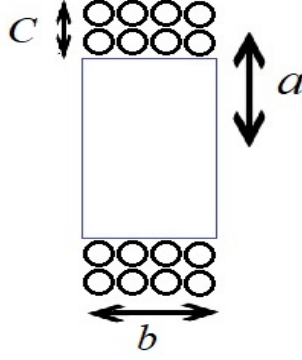


Figure 3.18: Cross section of multi-layer, multi-row coil

To calculate the inductance of the coils, Eq. (3.2) should be used where $a = 3.75$ cm (1.47 inches), $n = 60$ turns, $b = 3$ mm (0.11 inches) and $c = 3$ mm (0.11 inches), then the inductance (L) of coil will be 565mH.

Later in this thesis, the efficiency of the system will be calculated. Coil resistance is one of the parameters that needs to be calculated using the following equation [28]:

$$R_{\text{coil}} = \frac{a N}{\sigma r \delta} \quad (3.3)$$

where a is the highest radius of the transmitter or receiver coils (0.039 m), N is the number of turns for both coils (60 turns), σ is the conductivity of copper (5.8×10^7 S/m), r is the radius of the conductor (0.225×10^{-3} m) and δ is the skin depth.

Skin depth can be calculated, thus:

$$\delta = \frac{1}{\sqrt{\pi f \mu_0 \sigma}} \quad (3.4)$$

where f is a selected frequency (30,600 Hz), μ_0 the magnetic permeability of the air equaling $4\pi \times 10^{-7}$ H/m. Therefore, $\delta = 3.78 \times 10^{-3}$ μm . Finally, by using the above equations, the resistance of the transmitter coil $R_1 = 0.47\Omega$ and equally, the resistance of receiver coil $R_2 = 0.47\Omega$, which are the ohmic resistances of the coils.

An air core coil is commonly used in WPT systems because the current passing through it will never have an effect on its inductance and because it prevents the production of harmonics.

The optimization of the specifications of the coils in a WPT system has an important impact on the efficiency and distance of transferring power wirelessly. Normally, precise analysis of the ideal parameters of the coils is complicated since many factors affect the process of transformation. However, each application has its

own design requirements. For instance, to design implanted medical devices, and since they are inserted under the skin, the shape and size of the coils must be considered in the design. The two coils used in our design are shown in Figure 3.19.



(a)



(b)

Figure 3.19: Multi-layer, multi-row copper coil (a) The transmitter coil, and (b) The receiver coil

3.4 Summary

In this chapter, a block diagram of a WPT and its components from the DC power source to the load is explained and summarized. Table 3.1 shows every component that is used in the project.

Table 3.1: Components used in the design

Component's Name	Component's Value or code
Voltage Source, V_{DC}	9V and 15V
Capacitor, C1	100 μ F
Capacitor, C ₂	100nF
Capacitor, C3	47nF
Capacitor, C4	47nF
Capacitor, C5	100 μ F
Capacitor, C6	100 μ F
Capacitor, C7	100nF
Resistor, R1	410 Ω
Resistor, R2	220 Ω
Resistor, R3	220 Ω
Resistor, R4	470 Ω
Diode, D1	1N4733A
Diode, D2	SS36
Diode, D3	SS36
Diode, D ₄	LED
Diode, D5	W10M
PIC	PIC12F683
MOSFET, Q1	IRLZ44N
MOSFET, Q2	IRLZ44N
Voltage Regulator IC	LM7805
Push button Switch	SW
Transmitter coil, L ₁	565 μ H
Receiver coil, L ₂	565 μ H

CHAPTER FOUR

DESIGN AND IMPLEMENTATION OF WIRELESS POWER TRANSFER SYSTEM

4.1 Introduction

This chapter is an extension of the previous chapter. The design of our WPT system was implemented and all the components were collected to match all possible values of the proposed design, which will be the first design model. For our second model, a ferrite core will be used to enhance the efficiency of power transferal. These two WPT models were experimentally studied. The only difference between these two systems was the use of ferrite. However, theoretical calculations are described in this chapter in order to calculate the efficiency of the systems. Additionally, the relationship between the components of an RLC circuit is explained to match their values and to keep the system operating at the same resonance frequency.

4.2 Theoretical Model Calculation

As discussed previously, theoretical calculations are used during the design to optimize the performance of the WPT system, in addition to calculating the level of optimization, and evaluating the achievement of the final implementation.

4.2.1 The Conditions of Resonance in RLC Circuit

In the previous chapter, we demonstrated the value of the frequency used in our project, which was 30.6 kHz. However, the most important prerequisite for a WPT system is to improve the efficiency of the received power, which depends on increasing the quality factor Q . Referring back to Equation (2.16), it can be noticed that the quality factor varies with three parameters, such that it increases with an increase in

both the operation frequency and the inductance, and it decreases with an increase in equivalent resistance r_L . Therefore, the efficiency increases with the increase of the operation frequency, but the equivalent resistance will increase due to skin effect and proximity effect. Therefore, for each design, many parameters determine the quality of the system and there is an optimum frequency for every design. A new development by researchers for electric vehicles has been successful using a frequency of 20 kHz to charge their batteries wirelessly [29], while others prove that the optimum resonance frequency is approximately 100kHz [30].

When resonance occurs, the inductive reactance X_L of both circuits becomes equal to capacitive reactance X_C , then the reactive impedance become zero.

$$X_L = X_C \quad (4.1)$$

The resonance frequencies f_0 of the transmitter and receiver coils can be calculated as:

$$f_0 = \frac{1}{2\pi\sqrt{L_t C_t}} = \frac{1}{2\pi\sqrt{L_r C_r}} \quad (4.2)$$

In RLC circuits, the values of inductance and capacitance determine whether the RLC circuit works in resonance, which provides an area to make adjustments and balance between the values of L and C. However, it is necessary to keep the system operating at the same resonance frequency. Moreover, in the design, the frequency is set by the components of the circuit, such as the function generator or oscillator pulses generator, while the inductance is set according of the specifications of the coil. The matching capacitance value of the parasitic capacitor is a more straightforward approach to maintain the resonance frequency.

In our project, the resonance frequency used was 30.6 kHz and the inductance of the transmitter and receiver coils was 565 μ H, then, the capacitance of the inserted parasitic capacitors for both coils was 47nF.

4.2.2 Efficiency Formula

The transmitter and receiver coils must be linked with a strong magnetic coupling to have efficient power transfer over particular distances. The power transfer efficiency depends on the amount of power that is transferred from the transmitter part to the receiver part. Maximum efficiency occurs when the output voltage across load R_L is at maximum value. At the same time, the parasitic capacitance of the receiver

coil stores the maximum possible energy. Then the energy in the receiver coil reaches at maximum value. The system of wireless power transfer can be represented as a combination of elements, as shown in Figure 4.1. An equivalent circuit allows the calculation of the parameters of the circuit, such as voltage, current and efficiency.

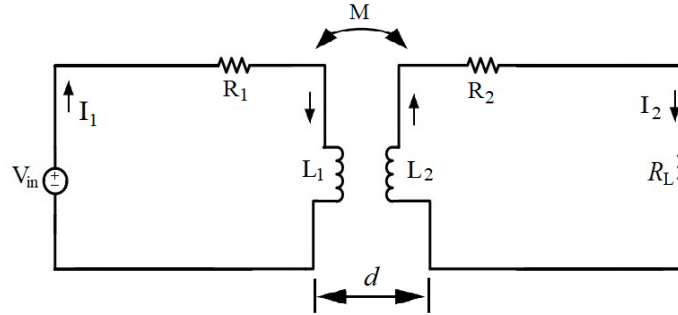


Figure 4.1: Equivalent circuit for theoretical model of WPT system

The transferred power to the load is a fraction of the input power. The transfer efficiency is given by the following equation [23] [31]:

$$\eta\% = \frac{\omega_0^2 M^2 R_L}{(R_2 + R_L)(R_1(R_2 + R_L) + \omega_0^2 M^2)} \quad (4.3)$$

where ω_0 is the angular frequency ($2\pi f_0$), and M the mutual inductance between the transmitter and receiver coils, which can be calculated using equation (2.13). R_L is the load resistance, R_1 and R_2 are the ohmic resistance of the transmitter and receiver coils respectively, they can be calculated using equations (3.3) and (3.4). From the above equation, the efficiency is related to the mutual inductance and the ohmic resistance of the transmitter and receiver coils, and the efficiency consider as transfer efficiency between the transmitter and the receiver coils.

The formula of efficiency might become more complicated when N number of receivers are coupled with one transmitter, such as when charging more than one portable device with one transmitter device. The efficiency of one receiver is affected by other receivers due to the mutual inductance of these receivers [32] and when one receiver is coupled to more than one transmitter such as when charging movable electric vehicles wirelessly could be complicated also. However, the all system efficiency is calculated by given equation:

$$\eta\% = \frac{P_o}{P_i} \quad (4.4)$$

Where p_o is a power dissipated by the load and P_i is a delivered power by the power source.

4.3 The Experimental Setup

In the previous chapter, we showed the block diagram of the wireless power transfer system and described the content and function of the elements of each block separately. The components of the entire system from end to end are compatible and integrated with each other and were chosen to achieve high performance. Herein, the system is ready to be set and merge together. The schematic diagram in Figures 4.2 and 4.3 show the entire transmitter and receiver circuits, respectively.

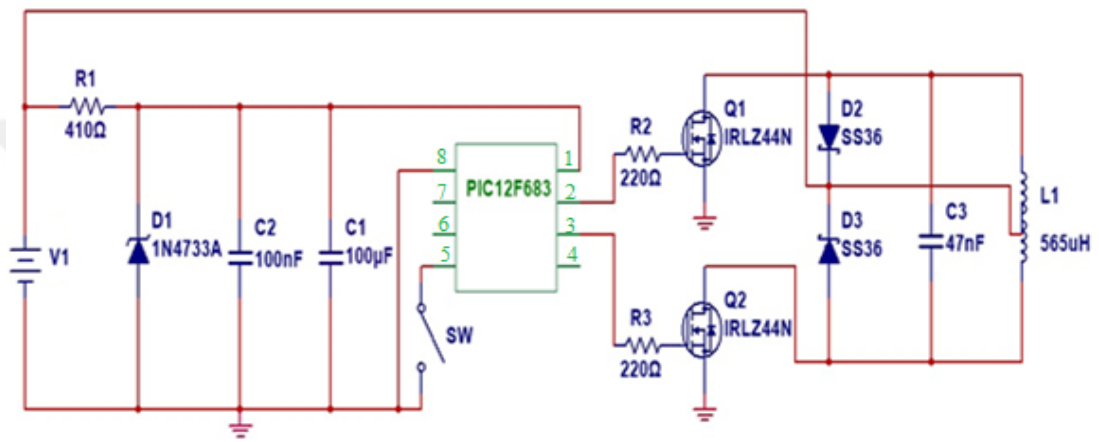


Figure 4.2: Circuit diagram of transmitter circuit

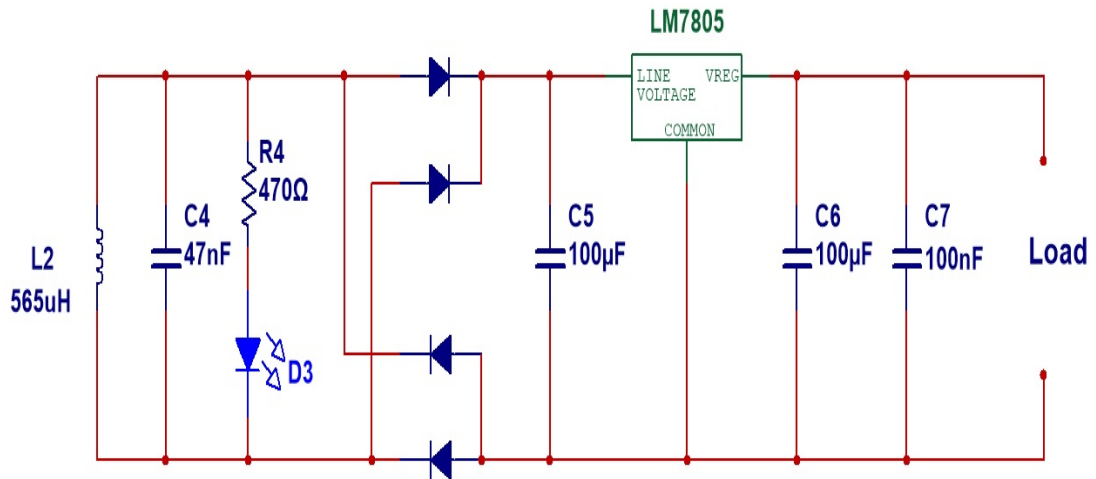


Figure 4.3: Circuit diagram of receiver circuit

Numerous tests were performed during the experimental work starting with the specifications of the coils, including their shape, number of turns, wire diameter, and diameter of the coils. Since the system operates in resonance with the combination of the inductance and capacitance, their values should be adjusted according to the Equation (3.1). It is important to optimize the coils' specifications based on the balance between the losses and the number of turns to obtain the desired amount of inductance for the coil that is tuned with the capacitor to obtain the resonance.

However, during the design stage, many different elements are used and many issues and challenges are encountered and should be overcome, such as the heat generated in the circuit due to high current flows, especially in MOSFETs. Moreover, tracing of the current flow and voltage drop is performed by placing an LED in the circuit with each step in order to help to indicate any open paths. Another challenge is short circuits, which are tested by using the buzzer of a multimeter device. Finally, a full evaluation is performed and printed circuit boards (PCBs) are made using the Proteus software program, see Figures (4.4) and (4.5) for the PCBs of the transmitter and receiver circuit, respectively. The dimensions of the transmitter PCB are 63mm × 32mm, while the dimensions of the receiver PCB are 66mm × 23mm.

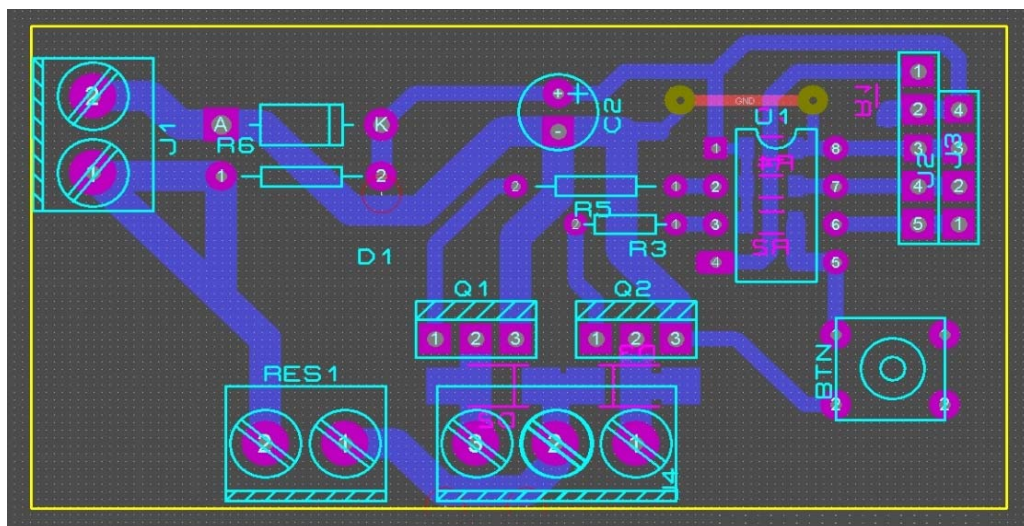


Figure 4.4: PCB layout design for transmitter circuit

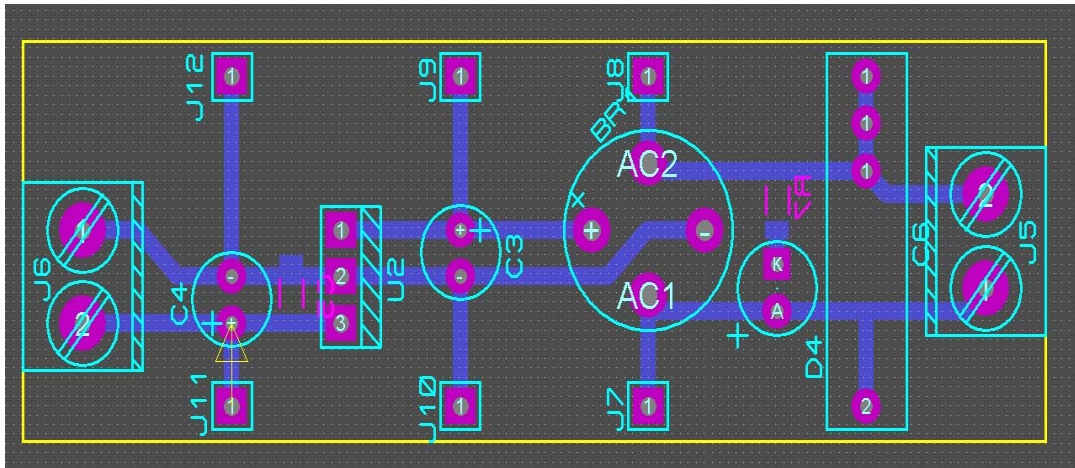


Figure 4.5: PCB layout design for the receiver circuit

As shown in figures (4.2 and 4.3), the input DC power sources used are 9 and 15 volts supplying the transmitter circuit. The Zener diode (D1) regulates the input voltage to 5.1V. Unwanted noise is eliminated by two filter capacitors (C1 and C2), followed by a more accurate direct voltage to a provided microcontroller chip circuit which works to generate high frequency pulses that will make the two MOSFETs (Q1 and Q2) work as switches to produce an AC signal and feed the transmitter coil (L1). Schottky diodes (D2 and D3) were used here to protect the MOSFETs from the back electromotive force. Capacitor (C3) makes the circuit operate with resonance. Now, according to Ampere's Circuital Law, a magnetic field is produced around the transmitter coil. According to Faraday's Law, this magnetic field interacts with the conductor to produce a current flow through it. Therefore, the receiver coil (L2) is placed near to L1 to have the system operate in an inductive coupling mode. Again, the capacitor (C4) has the receiver circuit tuned to resonance. The LED (D3) indicates an available magnetic coupling between the systems. The diode bridge rectifier converts the received AC signal into a DC signal. The capacitor (C5) acts to smooth the rippled signal. The regulated IC works to regulate the DC voltage at the desired amount. C6 and C7 work to eliminate unwanted high frequency noise. Fig. (4.6) shows the hardware setup of the system.

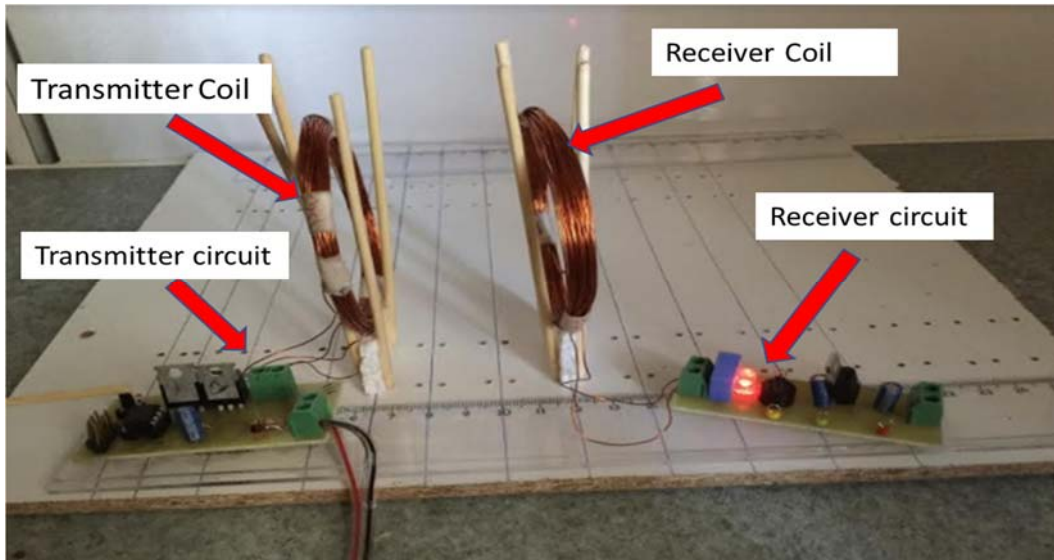


Figure 4.6: System hardware setup

CHAPTER FIVE

EXPERIMENTAL RESULTS AND DISCUSSION

5.1 Experimental Measurements Procedures

In this chapter, the results of the two implemented models will be verified and discussed. The first model is described in detail in the previous chapters and it will be referred to later in this chapter as a basic circuit design. The second model is identical to the first model, but ferrite material is used to improve the performance of the transmission and to increase the distance between the transmitter and receiver. The effects of ferrite will be studied followed by a presentation of a comparison between these two designs. Figure 5.1 shows the measurement set-up in the laboratory.

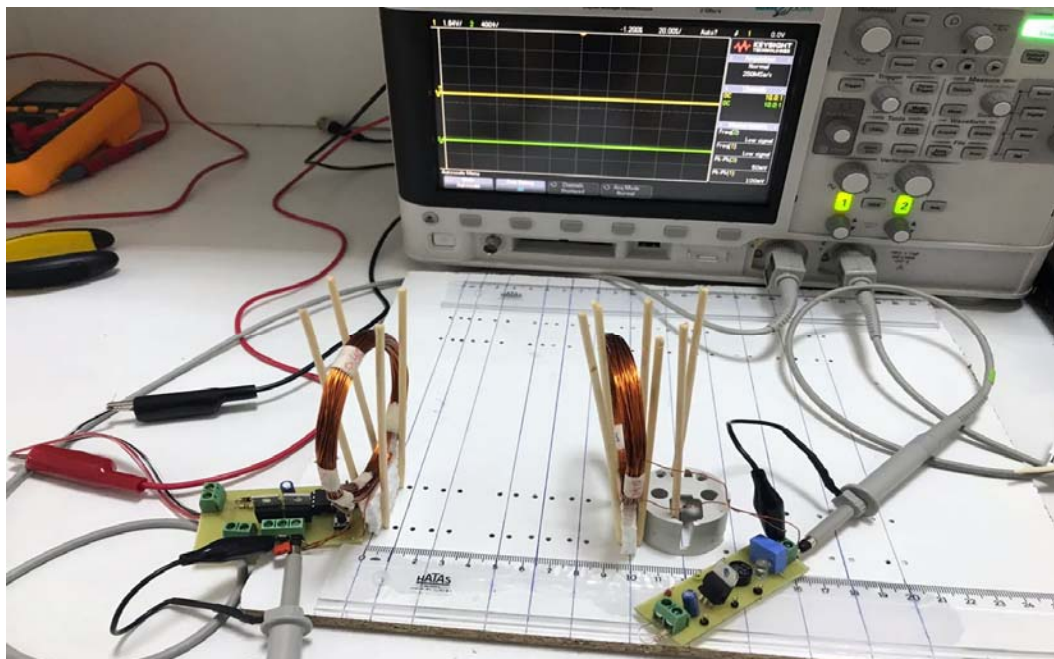


Figure 5.1: Measurement set-up in the laboratory

In the practical experiment, two sets of tests were measured:

1. Load resistance variation test

The load resistance variation test was performed in four sets using 9-volt and 15-volt of the input DC power in various combinations with distances $D = 25\text{mm}$ and $D = 65\text{mm}$. Also in each set, the load resistance values (R_L) were varied using the following resistances: $5\ \Omega$, $10\ \Omega$, $20\ \Omega$, $30\ \Omega$, $40\ \Omega$ and $50\ \Omega$. The power transfer efficiency was calculated with each resistance value to find the optimum values for the DC power supply and load resistances that produce higher efficiency. The charts show us the transfer efficiency according to the range of resistances that were used, which demonstrates the behavior of the system appropriate to a particular load. The above tests were performed without a ferrite core and with a ferrite core. Finally, comparisons between the results of measurements without and with the ferrite are presented.

2. Efficiency variation test

The efficiency variation test is performed as a comparison between the transfer efficiency of a WPT system with and without ferrite material. It is performed by varying the distance between the transmitter and receiver coil and by fixing the values of the load resistance and DC power supply according the optimum results achieved from the load resistance variation test. The chart shows the efficiency μ over distance D .

Before proccing the tests, numerous obtainable mathematically parameters should be computed to use them later for calculate the efficiency. The ohmic resistances of the transmitter and receiver coils (R_1 and R_2) are computed by using equation (3.3), which are equal to $0.47\ \Omega$, at each step of the measurement mutual inductance M is calculated by using equation (2.13). Finally, the efficiencies of the power transfer and the all system is calculated according to the load resistance R_L by using equation (4.3) and (4.4) respectively.

5.2 The Experimental Results of the Basic Circuit Design of WPT System

The measurements of the load resistance variation test were carried out with two values of the DC power supply, namely $V_{in} = 9\text{V}$ and $V_{in} = 15\text{V}$, and two distances between the transmitter and receiver coils, namely $D = 25\text{mm}$ and $D = 65\text{mm}$, and by varying the load resistance R_L between $5\ \Omega$ and $50\ \Omega$.

Table 5.1: Load resistance variation test of the basic circuit design when $V_{in}=9V$ $D=25mm$
 $R_{load} = 5-50\Omega$

Transmitter Circuit			Receiver Circuit				Efficiency	
V_{in} (V)	I_{in} (A)	P_{in} (W)	V_{out} (V)	I_{out} (A)	P_{out} (W)	R_{load} (Ω)	Transfer (%)	System (%)
9	0.82	7.38	2.5	0.5	1.25	5	89.2	16.9
9	0.82	7.38	2.47	0.24	0.61	10	87	8.2
9	0.81	7.29	2.34	0.11	0.27	20	85.8	3.7
9	0.81	7.29	2.19	0.06	0.15	30	83.3	2
9	0.8	7.2	2.05	0.04	0.1	40	79.7	1.4
9	0.8	7.2	1.94	0.03	0.07	50	76.2	0.97

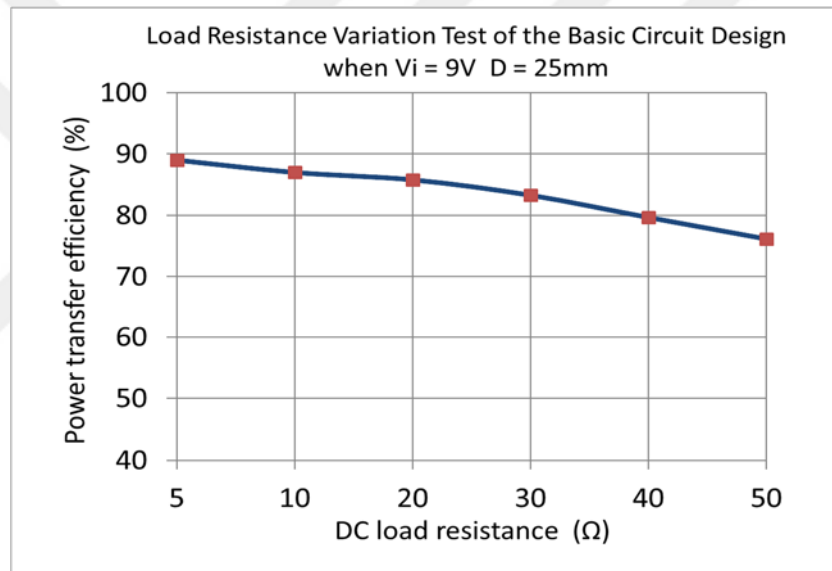


Figure 5.2: Load resistance variation test of the basic circuit design when $V_{in}=9V$ $D=25mm$ $R_{load} =5-50\Omega$

In this test, the optimum transfer efficiency is $\mu = 89.2\%$ when the load resistance $R_L = 5\Omega$, see Table 5.1 and Figure 5.2.

The same steps are repeated with the same distance ($D = 25\text{mm}$), but by setting the DC power supply to 15V and by varying the load resistance between 5Ω and 50Ω .

Table 5.2: Load resistance variation test of the basic circuit design when $V_{in}=15\text{V}$ $D=25\text{mm}$ $R_{load} = 5\text{-}50\Omega$

Transmitter Circuit			Receiver Circuit				Efficiency	
V_{in} (V)	I_{in} (A)	P_{in} (W)	V_{out} (V)	I_{out} (A)	P_{out} (W)	R_{load} (Ω)	Transfer (%)	System (%)
15	1.33	19.95	2.8	0.55	1.56	5	87.3	7.8
15	1.31	19.65	2.57	0.25	0.66	10	85.3	3.3
15	1.31	19.65	2.51	0.12	0.31	20	83.4	1.5
15	1.3	19.5	2.34	0.07	0.18	30	78.5	0.9
15	1.3	19.5	2.27	0.05	0.12	40	73.9	0.6
15	1.3	19.5	2.14	0.04	0.09	50	69.7	0.5

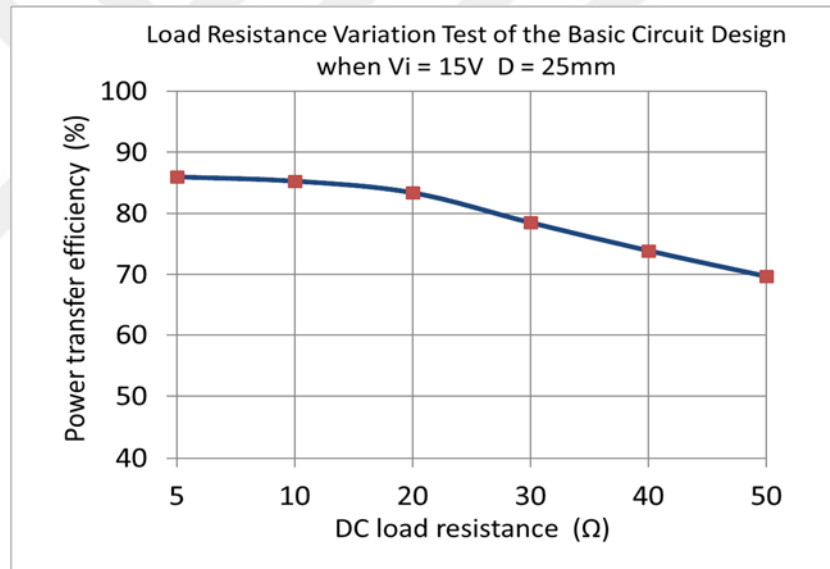


Figure 5.3: Load resistance variation test of the basic circuit design when $V_{in}=15\text{V}$ $D=25\text{mm}$ $R_{load} = 5\text{-}50\Omega$

The results of the load resistance variation tests of the basic circuit design, Tables 5.1 and 5.2 and Figures 5.2 and 5.3 show that when $D = 25\text{mm}$, optimum transfer efficiencies occur ($\mu = 89.2\%$ and $\mu = 87.3\%$) when $V_{in} = 9\text{V}$ and 15V respectively at a load resistance of 5Ω .

Now, we repeat the tests above but with an increase in the distance between the transmitter and receiver coils to $D = 65\text{mm}$. The input voltage is set to $V_{in} = 9\text{V}$ and the load resistance is varied between 5Ω and 50Ω .

Table 5.3: Load resistance variation test of the basic circuit design when $V_{in}=9\text{V}$ $D=65\text{mm}$ $R_{load} = 5\text{-}50\Omega$

Transmitter Circuit			Receiver Circuit				Efficiency	
V_{in} (V)	I_{in} (A)	P_{in} (W)	V_{out} (V)	I_{out} (A)	P_{out} (W)	R_{load} (Ω)	Transfer (%)	System (%)
9	0.81	7.29	1.77	0.35	0.62	5	80.5	8.5
9	0.8	7.2	1.76	0.17	0.3	10	75.9	4.1
9	0.8	7.2	1.75	0.08	0.15	20	65	2
9	0.79	7.11	1.73	0.05	0.1	30	56.3	1.4
9	0.79	7.11	1.71	0.04	0.07	40	49.6	0.9
9	0.78	7.02	1.71	0.02	0.03	50	44.2	0.4

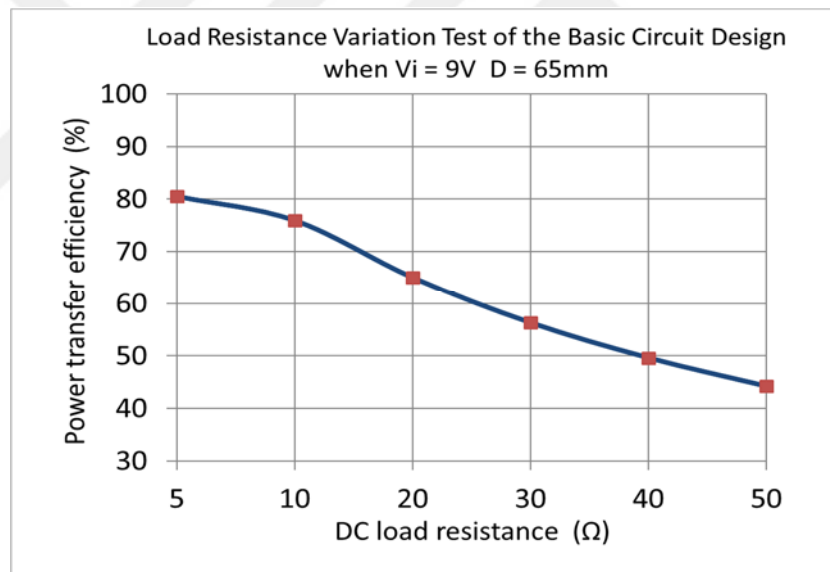


Figure 5.4: Load resistance variation test of the basic circuit design when $V_{in}=9\text{V}$ $D=65\text{mm}$ $R_{load} = 5\text{-}50\Omega$

Table 5.3 and Figure 5.4 show the results of load resistance variation test of the basic circuit design when $V_{in} = 9\text{V}$ and $D = 65\text{mm}$, the optimum efficiency occurs when $R_{load} = 5\Omega$ and by increasing the load, the efficiency constantly decreases.

Now, setting the DC power supply to $V_{in} = 15V$, the distance between the coils to $D = 65 \text{ mm}$ and varying the resistance of the load R_L between 5Ω and 50Ω .

Table 5.4: Load resistance variation test of the basic circuit design when $V_{in}=15V$ $D=65\text{mm}$ $R_{load} = 5-50\Omega$

Transmitter Circuit			Receiver Circuit				Efficiency	
V_{in} (V)	I_{in} (A)	P_{in} (W)	V_{out} (V)	I_{out} (A)	P_{out} (W)	R_{load} (Ω)	Transfer (%)	System (%)
15	1.32	19.95	1.88	0.38	0.71	5	76.3	3.5
15	1.3	19.5	1.88	0.19	0.35	10	69.3	1.8
15	1.3	19.5	1.87	0.09	0.17	20	56.1	0.8
15	1.28	19.2	1.87	0.06	0.12	30	46.8	0.6
15	1.28	19.2	1.87	0.05	0.09	40	40.1	0.5
15	1.27	19.05	1.86	0.04	0.07	50	35.1	0.4

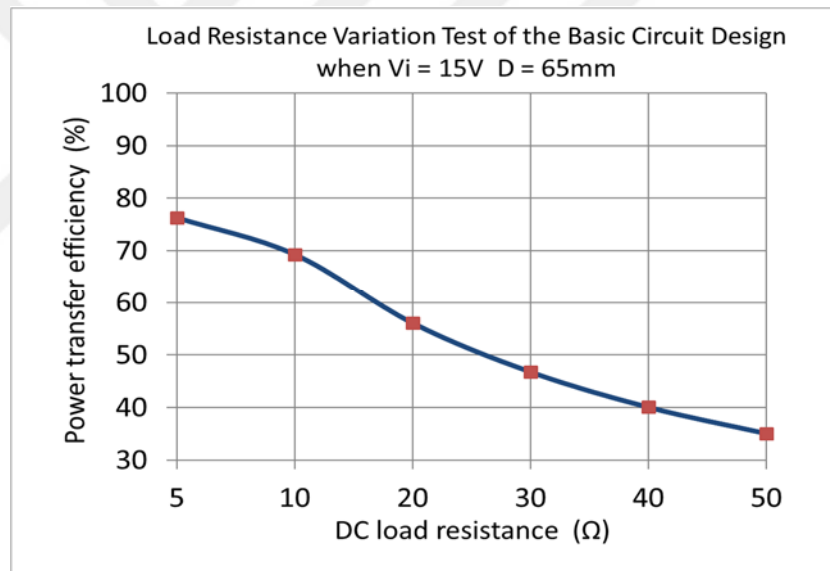


Figure 5.5: Load resistance variation test of the basic circuit design when $V_{in}=15V$ $D=65\text{mm}$ $R_{load} =5-50\Omega$

Table 5.4 and Figure 5.5 show the results of the load resistance variation tests of the basic circuit design at $V_{in} = 15V$ and $D = 65\text{mm}$, as a summary from the above four tests increasing both of the distance and the input DC voltage, the efficiency tends to decrease. Additionally, when the applied DC voltage is $9V$ and the distance between the coils is 25mm at a resistance load of 5Ω , the efficiency is optimal ($\mu = 89.2\%$), and by increasing the value of V_{in} from $9V$ to $15V$, the optimum efficiency decreases by 1.9% .

5.3 The Influence of Ferrite Materials

In experimental tests, soft ferrite material was used due to its characteristic features, such as its ability to change its magnetic properties according to the magnetic field that surrounds it. Normally, it has non-magnetic properties and cannot carry magnetism, however, when in a magnetic field, it tends to work as highly conductive ferromagnetic material. The type of ferrite material used in our project is manganese-zinc (Mn-Zn), which is commonly used in transformers due to its high magnetic permeability and high saturation. Soft ferrite materials come in different shapes and sizes, see Figure 5.6.

The advantage of using a ferrite material for wireless power transfer systems include:

1. Directing more of the magnetic field produced by the transmitter coil into the receiver coil.
2. Reducing the reluctance R_m (magnetic resistance) of the magnetic circuit.
3. Enhancing the mutual inductance M between the coupled coils.

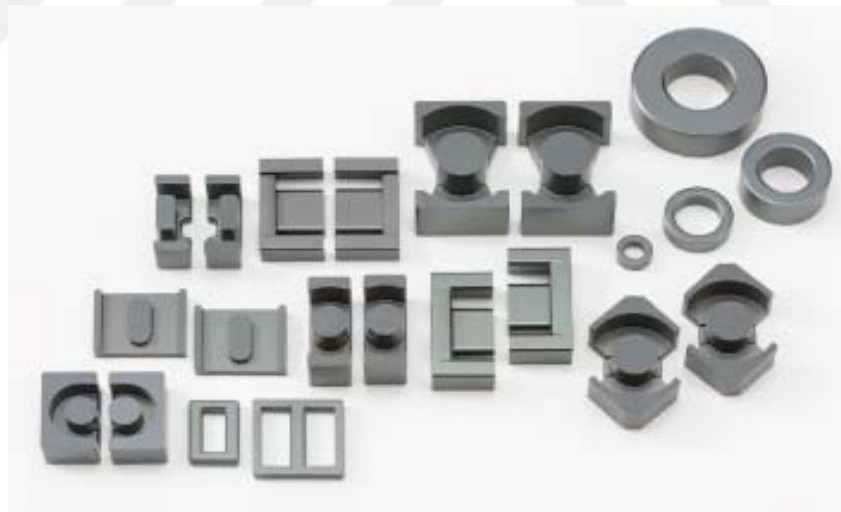


Figure 5.6: Various shapes and sizes of ferrite cores

The magnetic permeability of a material is defined as the ability to form and guide magnetic field lines toward a material located inside the field. Therefore, the magnetic resistance gets lower. However, passing the magnetic field through the ferrite leads to a reduction of the leakage flux, thereby increasing the magnetic flux density (Φ/m^2) near where the ferrite is placed.

In the experimental tests, the soft ferrite core was placed behind the receiver coil, see Figure 5.7.

The use of Mn-Zn ferrite in our project was based on increasing the mutual inductance between the transmitter and receiver coils since this material has high magnetic permeability at a low frequency thereby influencing the magnetic field [33] so that the magnetic field is concentrated and attracted into it.

The increment of the magnetic flux density in the area of receiver coil leads to an increase in the coupling coefficient K , and thus an increase in both of the transfer efficiency and the all system efficiency.

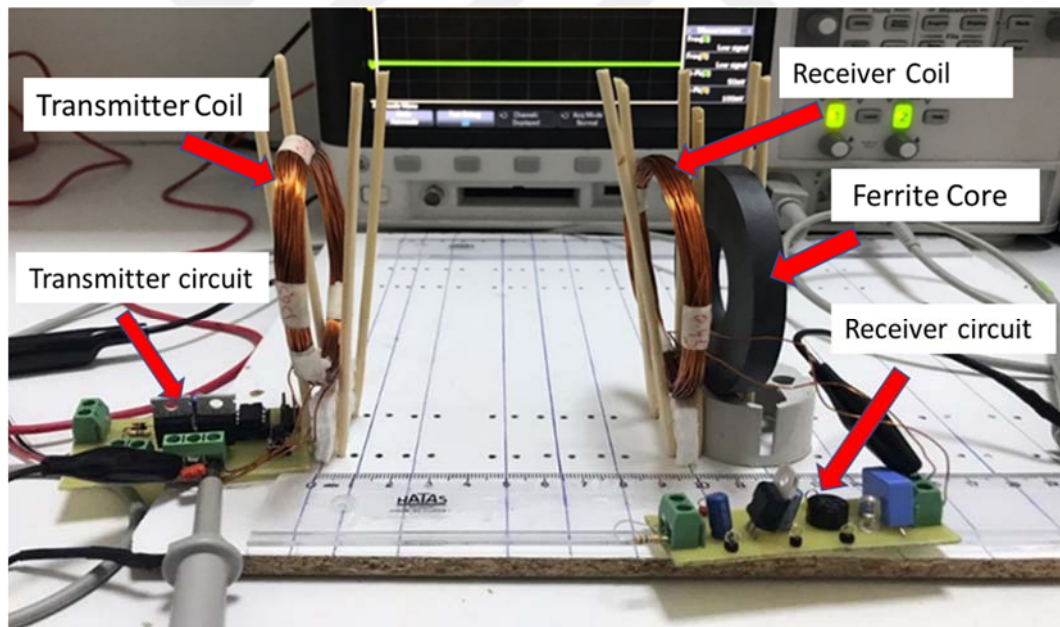


Figure 5.7: Ferrite core during experimental tests

5.4 The Experimental Results of the Design With Using Ferrite of WPT System

The measurements of the load resistance variation test were performed by putting a soft ferrite core behind the receiver coil, see Figure 5.7. The same tests were performed in section 5.2 will repeated.

Table 5.5: Load resistance variation test with using ferrite when $V_{in}=9V$ $D=25mm$ $R_{load} = 5-50\Omega$

Transmitter Circuit			Receiver Circuit				Efficiency	
V_{in} (V)	I_{in} (A)	P_{in} (W)	V_{out} (V)	I_{out} (A)	P_{out} (W)	R_{load} (Ω)	Transfer (%)	System(%)
9	0.81	7.29	2.6	0.5	1.35	5	90.9	18.6
9	0.81	7.29	2.53	0.24	0.64	10	89.5	8.8
9	0.81	7.29	2.46	0.11	0.3	20	88.9	4.1
9	0.8	7.2	2.17	0.06	0.16	30	85.8	2.2
9	0.8	7.2	2.09	0.04	0.11	40	82.7	1.5
9	0.8	7.2	2.06	0.3	0.08	50	79.6	1.1

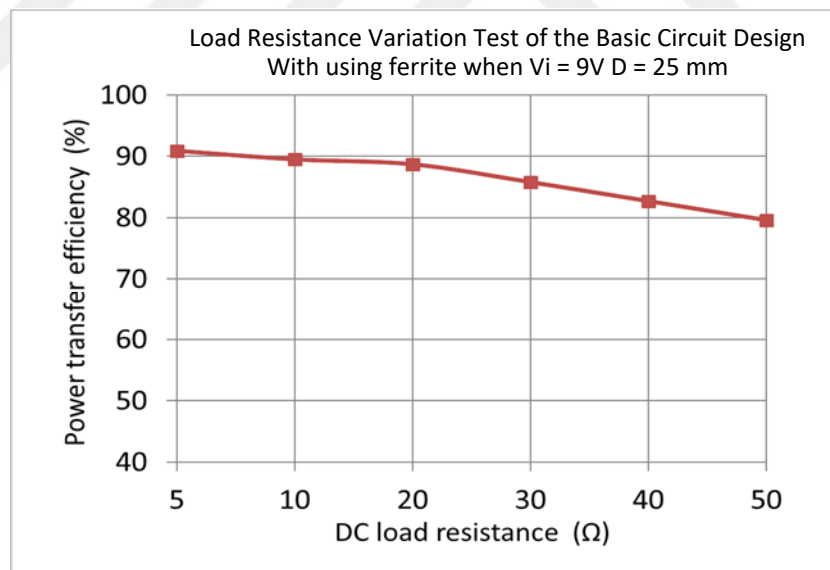


Figure 5.8: Load Resistance Variation with using ferrite when $V_{in}=9V$ $D=25mm$ $R_{load} =5-50\Omega$

In this test, the optimum transfer efficiency is ($\mu=90.9\%$) when the load resistance $R_L=5\Omega$, see Table 5.5 and Figure 5.8.

The same previous test repeats with the same distance $D = 25 \text{ mm}$, but the input voltage is $V_{in}=15\text{V}$ and the varying load resistance is $5\text{-}50 \Omega$ with the ferrite.

Table 5.6: Load resistance variation test with using ferrite when $V_{in}=15\text{V}$ $D=25\text{mm}$ $R_{load} = 5\text{-}50\Omega$

Transmitter Circuit			Receiver Circuit				Efficiency	
V_{in} (V)	I_{in} (A)	P_{in} (W)	V_{out} (V)	I_{out} (A)	P_{out} (W)	R_{load} (Ω)	Transfer (%)	System (%)
15	1.31	19.65	2.92	0.58	1.7	5	89	8.6
15	1.3	19.5	2.66	0.27	0.71	10	88.2	3.6
15	1.3	19.5	2.62	0.13	0.34	20	85.6	1.7
15	1.29	19.35	2.46	0.08	0.2	30	81.3	1
15	1.27	19.05	2.29	0.06	0.13	40	77.2	0.6
15	1.27	19.05	2.15	0.04	0.09	50	73.4	0.4

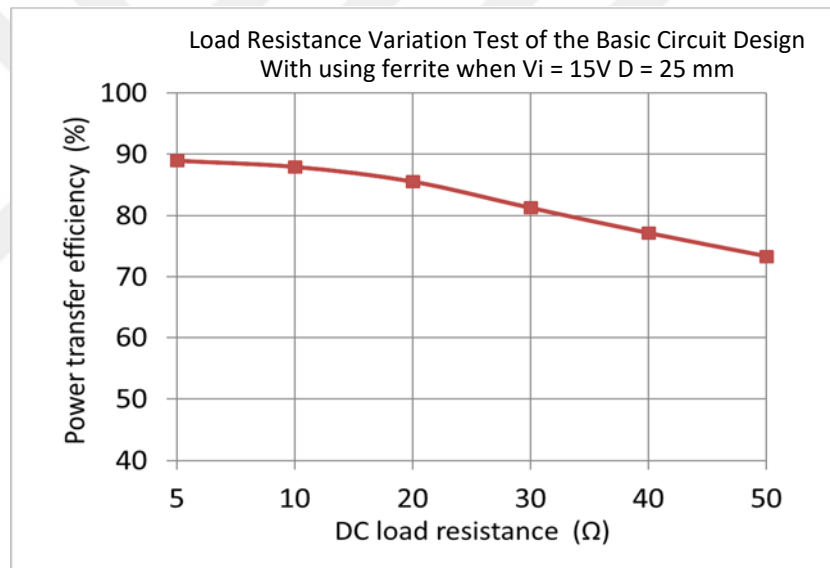


Figure 5.9: Load resistance variation with using ferrite when $V_{in}=15\text{V}$ $D=25\text{mm}$ $R_{load} =5\text{-}50\Omega$

By using ferrite core in basic circuit design, Tables 5.5 and 5.6 and Figures 5.8 and 5.9 show that when $D = 25\text{mm}$, $V_{in} = 9\text{V}$ and the load resistance $R_{load} = 5\Omega$, the optimum efficiency occurs ($\mu = 90.9\%$), it is obvious that the input voltage $V_{in} = 9\text{V}$ is considered an optimum input voltage.

Here, we use the ferrite again and make the distance between the transmitter and receiver coils $D = 65\text{mm}$, input voltage $V_{in} = 9\text{V}$ and we vary the load resistance $R_{load} = 5\text{-}50\ \Omega$.

Table 5.7: Load resistance variation test with using ferrite when $V_{in}=9\text{V}$ $D=65\text{mm}$ $R_{load} = 5\text{-}50\Omega$

Transmitter Circuit			Receiver Circuit				Efficiency	
V_{in} (V)	I_{in} (A)	P_{in} (W)	V_{out} (V)	I_{out} (A)	P_{out} (W)	R_{load} (Ω)	Transfer (%)	System (%)
9	0.8	7.2	1.78	0.35	0.63	5	84	8.7
9	0.8	7.2	1.77	0.17	0.31	10	81.8	4.3
9	0.8	7.2	1.77	0.09	0.16	20	73.6	2.2
9	0.78	7.02	1.75	0.06	0.1	30	66.2	1.4
9	0.78	7.02	1.72	0.04	0.07	40	60	1
9	0.78	7.02	1.71	0.03	0.06	50	54.9	0.8

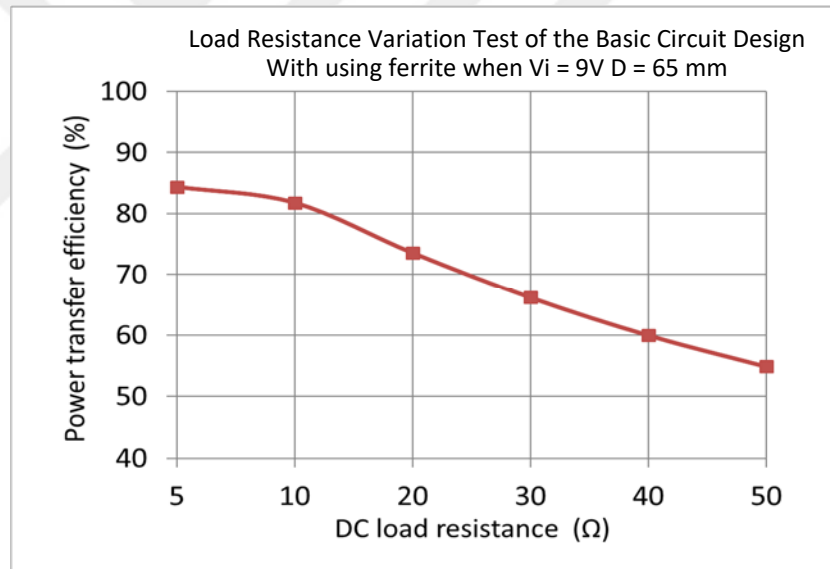


Figure 5.10: Load resistance variation test with using ferrite when $V_{in}=9\text{V}$ $D=65\text{mm}$ $R_{load} = 5\text{-}50\Omega$

The results of the load resistance variation test with the ferrite when $V_{in} = 9\text{V}$, $D = 65\text{mm}$, Table 5.7 and Figure 5.10 show that the optimum transfer efficiency ($\mu = 84\%$) occurs when $R_{load} = 5\Omega$. With an increase in the load, the efficiency constantly decreases.

Now, we set the DC power supply to $V_{in} = 15V$, the distance between the coils to $D = 65mm$ and we vary the load resistance $R_{load} = 5-50\Omega$.

Table 5.8: Load resistance variation test with using ferrite when $V_{in}=15V$ $D=65mm$ $R_{load} = 5-50\Omega$

Transmitter Circuit			Receiver Circuit				Efficiency	
V_{in} (V)	I_{in} (A)	P_{in} (W)	V_{out} (V)	I_{out} (A)	P_{out} (W)	R_{load} (Ω)	Transfer (%)	System (%)
15	1.31	19.65	1.89	0.38	0.71	5	79.9	3.6
15	1.3	19.5	1.88	0.19	0.35	10	75	1.7
15	1.29	19.35	1.88	0.1	0.18	20	63.6	0.9
15	1.28	19.2	1.88	0.06	0.12	30	54.8	0.6
15	1.27	19.05	1.87	0.06	0.09	40	48	0.5
15	1.27	19.05	1.87	0.04	0.07	50	42.7	0.4

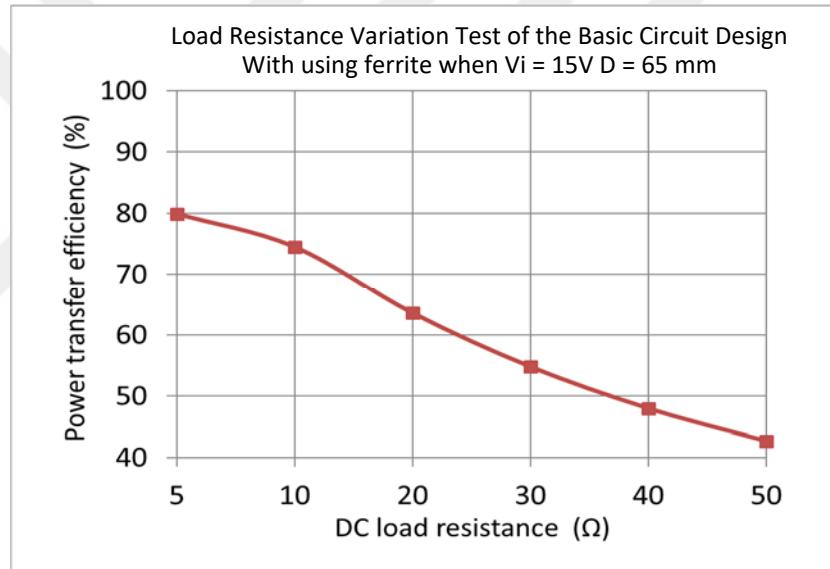


Figure 5.11: Load resistance variation test with using ferrite when $V_{in}=15V$ $D=65mm$ $R_{load} = 5-50\Omega$

The results of the load resistance variation tests with using ferrite when $V_{in} = 15V$ and $D = 65mm$, Table 5.8 and Figure 5.11 show that with an increase in both the distance and input DC voltage, the efficiency decreases.

As a summary from above four tests, using ferrite when the DC input voltage is 9V and the distance between the coils is 25 mm at a resistance load of 5 Ω , the efficiency is optimal ($\mu=90.9\%$), and by increasing the value of V_{in} from 9V to 15V at $D = 25mm$, the optimum efficiency decreases approximately 2%. And similarly, at $D = 65mm$ the optimum efficiency decreases approximately 4% when $V_{in} = 15V$ than $V_{in} = 9V$.

5.5 Results Comparison With and Without Using Ferrite

In this section, the experimental test results of the basic circuit design with and without using the ferrite core are compared. The parameters of the comparisons are taken from the results of the experimental tests made previously.

5.5.1 Results Comparison of the Load Resistance Variation Test

The parameters of the following comparisons are taken from the results of the experimental tests made previously. The comparisons are made to show the optimum efficiency with respect to the input voltage of the proposed circuit design and also to show the influence of the ferrite core on efficiency.

When $V_{in} = 9V$, $D = 25mm$ and varying the load resistance $R_L = 5-50 \Omega$.

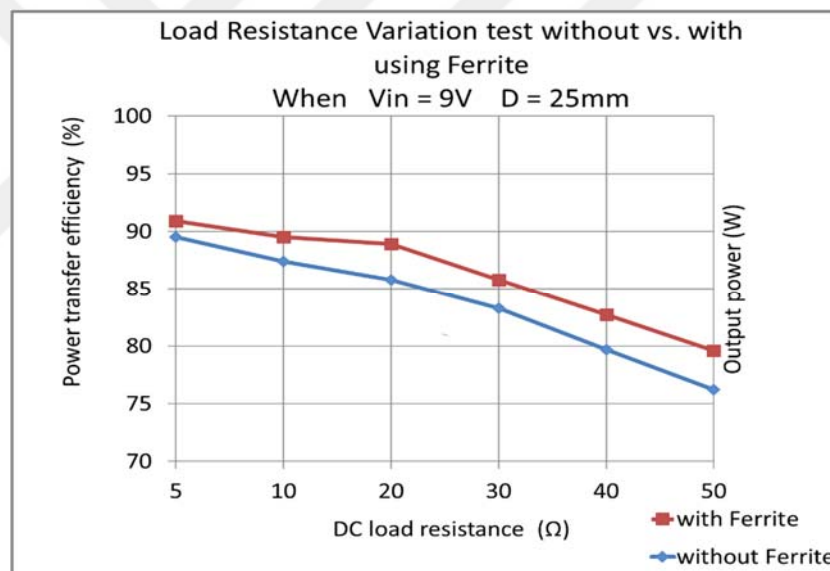


Figure 5.12: Comparison of the load resistance variation test with and without using ferrite when $V_{in}=9V$ $D=25mm$ $R_{load} = 5-50\Omega$

The load resistance variation test of both the basic circuit design with and without the ferrite core is shown in Figure 5.12. The chart shows that when $V_{in} = 9V$ and $D = 25mm$, the model with the ferrite reaches 1.7% higher maximum efficiency than without using the ferrite core. Moreover, the increment of efficiency appears clearly when the load resistance increases.

When $V_{in} = 15V$, $D = 25mm$ and varying the load resistance $R_L = 5-50 \Omega$

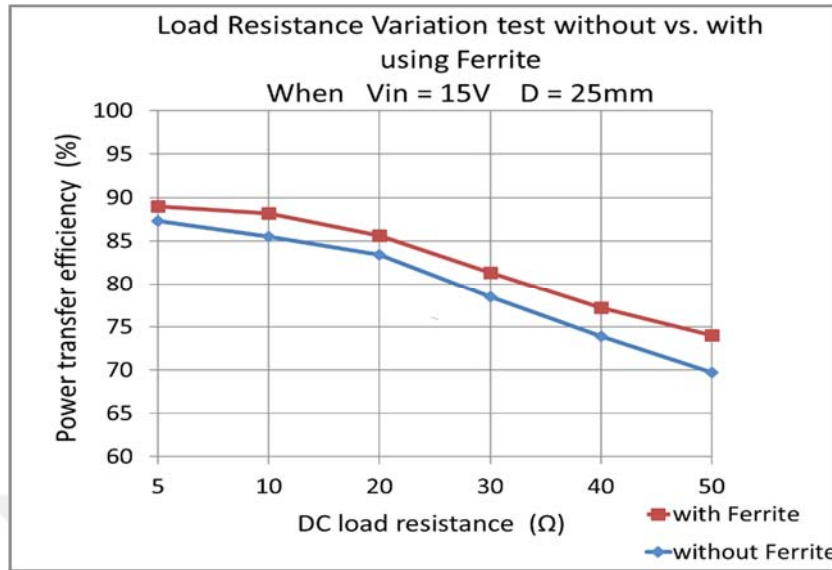


Figure 5.13: Comparison of the load resistance variation test with and without using ferrite when $V_{in}=15V$
 $D=25mm$ $R_{load} = 5-50\Omega$

Figure 5.13 shows when $R_L = 5\Omega$ that gives a higher efficiency value for both two models.

When $R_L = 5\Omega$, the ferrite enhances the efficiency by 1.7%, but when $R_L = 50 \Omega$, the efficiency is enhanced by 3.7%.

Figures 5.12 and 5.13 show the optimum efficiency when $V_{in} = 9V$ is higher than when $V_{in} = 15V$, whether or not the ferrite core was used.

When $V_{in} = 9V$, $D = 65mm$ and varying the load resistance $R_L = 5-50\Omega$.

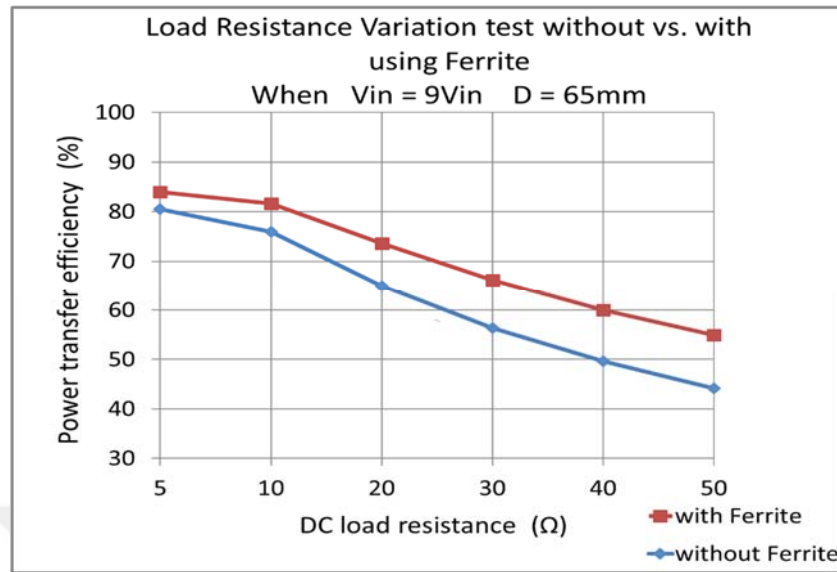


Figure 5.14: Comparison of the load resistance variation test with and without ferrite when $V_{in} = 9V$ $D = 65mm$ $R_{load} = 5-50 \Omega$

Figure 5.14 shows that when the input voltage $V_{in} = 9V$ and $D = 65mm$, the enhanced efficiency is higher than when $D = 25mm$ with the same DC power supply, that indicates using ferrite at further distance between the transmitter and the receiver coils has a major influence on efficiency than closer distance, furthermore, the enhanced efficiency increases commensurately with an increase in the load resistance. The optimum efficiency for the two models occurs when $R_L = 5\Omega$, using ferrite at this load enhances the efficiency by 3.5%, but when $R_L = 50\Omega$, the ferrite enhances the efficiency by 10.7%.

When $V_{in} = 15V$, $D = 65mm$ and varying the load resistance $R_L = 5-50\Omega$

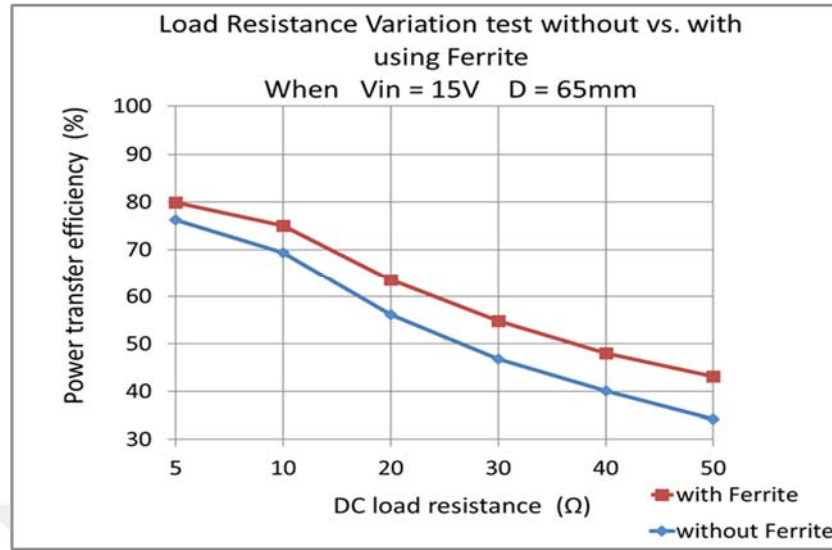


Figure 5.15: Comparison of the load resistance variation test with and without using ferrite when $V_{in}=15V$ $D=65mm$ $R_{load} = 5-50\Omega$

Figure 5.15 shows the optimum efficiency for the two models occurring when $R_L = 5\Omega$. Additionally, at this load, the ferrite increases the efficiency by 3.6%, while, when $R_L = 50\Omega$, the ferrite the efficiency rises to 7.6%.

The comparisons show that with an increase in the load resistance, an enhanced efficiency was higher with the ferrite. Moreover, when the load resistance was lower, the efficiency increased only slightly by using ferrite.

The optimum efficiency when $V_{in} = 9V$ is higher than when $V_{in} = 15V$, whether or not the ferrite is used.

5.5.2 Comparing the Transfer Efficiency over Distance

The previous tests were carried out with two distances between the transmitter and receiver coils, namely $D = 25mm$ and $D = 65mm$, and two DC power supplies namely $V_{in} = 9V$ and $V_{in} = 15V$, to determine which power supply attain the highest efficiency. The pervious results show the optimum efficiency occurs when the DC power supply $V_{in} = 9V$, and load resistance $R_{load} = 5\Omega$. Therefore, in the next test, the value of the DC power supply set to $V_{in} = 9V$, and the load resistance fix to $R_L = 5\Omega$, furthermore, the distance was varied between 10mm and 380mm to determine the influence of the ferrite over the distance. The next chart shows that when D increases, the increment of efficiency appears clearly with using ferrite.

Table 5.9: Comparing the efficiency over the distance with and without using ferrite when $V_{in}=9V$
 $D=10-380mm$ $R_{load} = 5\Omega$

D (mm)	10	25	65	100	140	180	220	260	300	340	380
$\mu_{without}$ (%)	90.8	89.2	80.5	78	72.3	23.5	7	0.2	0	0	0
μ_{with} (%)	92	90.9	84	82.3	80.3	74	66.6	38	14.5	2.5	0.3

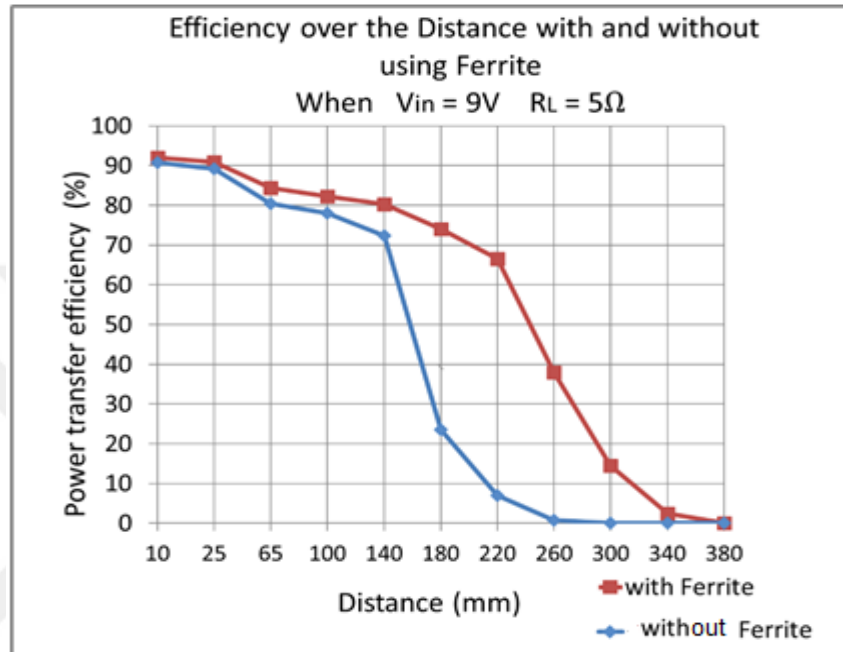


Figure 5.16: Comparing the transfer efficiency over the distance with and without using ferrite when $V_{in}=9V$ $D=10-380mm$ $R_{load} = 5\Omega$

During the measurements, the distance was increased gradually until the efficiency became zero. Table 5.9 and Figure 5.16 show the performance of the system with and without using the ferrite core. When the system working without the ferrite at $D = 140mm$, the efficiency decreased rapidly, and up to $D = 220mm$, the efficiency was insignificant and the transferred power becoming useless. However, when using the ferrite core, the efficiency began to decrease rapidly at $D = 220mm$ and when approaching $D = 320mm$, the efficiency became useless.

It is obvious from the above chart that when the transmitter and receiver coils are close to each other ($D < 140mm$), the influence of the ferrite becomes insignificant because within this region, the magnetic field is concentrated and the mutual inductance is at maximum value. However, by increasing the distance between the coils, the magnetic flux begins to scatter all around and only a small portion of it arrives at the receiver coil. Hence, in this case, the ferrite core becomes useful and important

to collect this scattered flux and direct it into the receiver coil resulting in the efficiency of transferred power being maintained even with increases in distance between the coils. It can be seen from Figure 5.16 that the ferrite core enhanced the power transfer efficiency and when using the ferrite at $D = 180\text{mm}$, the efficiency was able to reach approximately 50% higher than without using it. At $D = 220\text{mm}$, the efficiency reached approximately 60% higher than without the ferrite.

It is essential to mention that during experimental tests at certain long distances between coils, even though the efficiency reaches almost zero, a voltage is produced in the receiver circuit. To illustrate, in the design without the ferrite at $D = 300\text{mm}$, the voltage was measured to be $V = 0.1\text{V}$, and for the design with using the ferrite at $D = 460\text{ mm}$, the voltage also measured at $V = 0.1\text{V}$. These are not effective and we are unable to use it for charging batteries or other wireless power transfer applications. However, that implies the existence of mutual inductance even of only a few picofarads.

CHAPTER SIX

CONCLUSIONS AND FUTURE WORK

6.1 Conclusion

The design and implementation of this project was concerned with the principle of inductive resonance coupling of a WPT between the transmitter and receiver circuits. The increasing use of portable devices and the development of their new technology cause us to find ways to use them with more mobility while they are charging. As a result, charging them wirelessly is the new upcoming technology. At the beginning of this project, the focus was to use most of the magnetic field generated by the transmitter coil to obtain higher delivered power at the receiver coil. Our project was divided into nine blocks, starting from the power supply and ending at the load. The compatibility of the elements used was studied in terms of avoiding any mismatches between them and other block elements. Then, the equivalent circuit of the WPT system was defined to simplify the theoretical calculations, including the ohmic resistance, the inductance of the coils, the values of the parasitic capacitors, the mutual inductance and the efficiency.

Ampere's Circuital Law states that when electric current passes through a conductor, it produces a magnetic field around it. This field scatters around the ambient area of the transmitter coil. Here, our challenge was to collect this dispersed magnetic field and directed it into a receiver coil and utilize the maximum possible field. The material of high magnetic permeability being used was a soft ferrite core.

Experimental tests show that using a ferrite core improves efficiency and increases the distance between the transmitter and receiver coils, the transfer efficiency of the system at $D = 180\text{mm}$, improving from 23.5% to 74% when using a ferrite core.

The optimum voltage source was measured to be $V_{in} = 9V$. The optimum load resistance was $R_L = 5\Omega$. Table 6.1 below shows the maximum efficiency values achieved for both circuits at two different distances (D) between the coils.

Table 6.1: Maximum Efficiencies of the WPT System with and without using Ferrite

	μ (%) when D=25mm $V_{in} = 9V$	μ (%) when D=65mm $V_{in} = 9V$
without using ferrite	89.2	80.5
with using ferrite	90.9	84

6.2 Future Work

Based on the results achieved from the experimental tests, a lot of work must be done to improve the performance of WPT systems. Increasing consumer convenience is a goal when designing most WPT systems, according to the criteria listed below:

1. Decrease the volume of the system and the ferrite core.
2. Increase the distance between the transmitter and receiver coils.
3. Increase delivered power to the load.
4. Expanding the study of influence of ferrite materials.
5. Investigating the use of two coils in receiver circuit and one coil in transmitter circuit.
6. Using MOSFETs Driver for driving the gate of MOSFETs to reduce of power dissipation.

REFERENCES

- [1] Caty Fairclough, “Investigating Wireless Power Transfer with Simulation,” Comsol blogs, Available online at: https://www.comsol.com/blogs/investigating-wireless-power-transfer-with-simulation/?utm_content=buffer80908&utm_medium=Social&utm_source=Twitter&utm_campaign=comsol_social_pages
- [2] International Telecommunication Union (ITU), “Applications of wireless power transmission via radio frequency beam,” *Report ITU-R SM.2392-0* (08/2016).
- [3] Maqsood, M. and Nauman Nasir, M. (2013), “Wireless electricity (Power) transmission using solar based power satellite technology,” *Journal of Physics, Conference Series 439 012046*, (2013).
- [4] B.-J. Jang, S. Lee, and H. Yoon, “HF-Band Wireless Power Transfer System: Concept, Issues, and Design,” *Progress in Electromagnetics Research*, Vol. 124, 211-231, 2012.
- [5] Kurs, A., A. Karalis, R. Moffatt, J. D. Joannopoulos, P. Fisher, and M. Soljagic, “Wireless power transfer via strongly coupled magnetic resonances,” *Science*. 317, pp83-86, Jul. 2007.
- [6] Dickinson, R. M., “Performance of a high-power, 2.388-GHz receiving array in wireless power transmission over 1.54km”, 1976 MTT-S Int. Microwave Symp. Digest, pp.139-141, 1976.
- [7] Gopinath, Ashwin, “All About Transferring Power Wirelessly,” *Electronics for You*, EFY Enterprises Pvt. Ltd, 52-56, August 2013.
- [8] John Markoff, “Intel Moves to Free Gadgets of Their Recharging Cords,” 20 August 2008, Available online: <http://www.nytimes.com/2008/08/21/technology/21intel.html?mcubz=0>
- [9] Intel Corporation website, Wireless Power – Wireless Resonant Energy Link (WREL), July 1, 2010, Available online: <https://newsroom.intel.eu/chip-shots/wireless-power-wireless-resonant-energy-link-wrel/>

- [10] Karalis, A., Kurs, A., Moffatt, R., Joannopoulos, J., Fisher, P., and Soljacic, M. (2010). "Wireless power range increase using parasitic resonators," *US Patent App.* 12/787,765.
- [11] Kiani, M. and Ghovanloo, M. (2013). "A figure-of-merit for designing high performance inductive power transmission links." *Industrial Electronics, IEEE Transactions on*, 60(11):5292–5305.
- [12] RamRakhyani, A. K. and Lazzi, G. (2013). "On the design of efficient multi-coil telemetry system for biomedical implants." *Biomedical Circuits and Systems, IEEE Transactions on*, 7(1):11–23.
- [13] Lee, K. and Cho, D. (2015). "Analysis of wireless power transfer for adjustable power distribution among multiple receivers," *Antennas and Wireless Propagation Letters, IEEE Transactions on*, vol.14, pp. 950 – 953.
- [14] Jiwarivavej, V., Imura, T., and Hori, Y. (2014). "Coupling Coefficients Estimation of Wireless Power Transfer System via Magnetic Resonance Coupling Using Information from Either Side of the System," *IEEE, Journal of Emerging and Selected Topics in Power Electronics (Volume: 3, Issue: 1, pp 191-200, March 2015.*
- [15] Vijayakumaran Nair, Vijith, Choi, and Jun R. 2016. "An Efficiency Enhancement Technique for a Wireless Power Transmission System Based on a Multiple Coil Switching Technique," *Energies* 9, no. 3: 156
- [16] Malisuwan, S., Tiamnara, N and Suriyakrai, N., "Design of Antennas for a Rectenna System of Wireless Power Transfer in the LTE/WLAN Frequency Band," *Journal of Clean Energy Technologies*, Vol. 5, No.1, pp. 42-46, January 2017.
- [17] Poon, A. S., O'driscoll, S., and Meng, T. H. (2007). "Optimal operating frequency in wireless power transmission for implantable devices," *EMBS 2007. 29th annual international conference of the IEEE*, pp 5673–5678.
- [18] Vrushali B. Gore and Dhanashri H. Gawali (2016). "Wireless Power Transfer Technology for Medical Applications," *2016 Conference on Advances in Signal Processing (CASP) Cummins College of Engineering for Women, Pune. Jun 9-11, 2016 pages 455-460.*
- [19] Jaechun Lee and Sangwook Nam (2010). "Fundamental Aspects of Near-Field Coupling Small Antennas for Wireless Power Transfer," *transactions on antennas and propagation*, IEEE, vol. 58, no. 11, November 2010 pages 3442-3449.

- [20] Xiaoming Chen, Zhaoyang Zhang, Hsiao-Hwa Chen, and Huazi Zhang (2015). “Enhancing Wireless Information and Power Transfer by Exploiting Multi-Antenna Techniques,” *energy harvesting communications*, IEEE, Communications Magazine, April 2015, pages 133-141.
- [21] C. Alexander and M. Sadiku., “Fundamentals of Electric Circuits,” *McGraw-Hill*, 2nd edition, 2003.
- [22] K. Bong Kim, E. Levi, Z. Zabar and L. Birenbaum, “Mutual Inductance of Noncoaxial Circular Coils with Constant Current Density, +” *IEEE Transactions on Magnetics*, VOL. 33, NO. 5, September 1997.
- [23] Y. Han and X. Wang, “Calculation of Mutual Inductance Based on 3D Field and Circuit Coupling Analysis for WPT System,” *International Journal of Control and Automation*, Vol. 8, No. 4 (2015), pp. 251-266.
- [24] U.S. Gudmundsdottir, “Proximity effect in fast transient simulations of an underground transmission cable,” *Electric Power Systems Research*. (2014).
- [25] Xuezhe W., Zhenshi W., and Haifeng D., “A Critical Review of Wireless Power Transfer via Strongly Coupled Magnetic Resonances,” *Energies*, ISSN 1996-1073, pp 4316-4341,2014.
- [26] O. Jonah, V. Georgakopoulos, M. M. Tentzeris, “Optimal Design Parameters for Wireless Power Transfer by Resonance Magnetic,” *IEEE Antennas and wireless propagation letters*, pp.1390-1393 vol. 11, 2012.
- [27] F.E. Terman, *Radio Engineers' Handbook*, McGraw-Hill, New York, 1943, p.62.
- [28] B. L. Cannon, J. F. Hoburg, and D. D. Stancil, “Magnetic Resonant Coupling as a Potential Means for Wireless Power Transfer to Multiple Small Receivers,” *IEEE Transactions on Power Electronics*, vol. 24, no. 7, July 2009.
- [29] Song, B. M., R. Kratz, and S. Gurol, “Contactless inductive power pickup system for maglev applications,” *IEEE Transactions on Industry Applications Proc. Conf. 37th IAS, Ann. Meeting*, Vol. 3, 1586–1591, 2002.
- [30] R. Mecke and C. Rathage, “High frequency resonant inverter for contactless energy transmission over large air gap,” *Proc. IEEE-PESC* 1, 1737–1743 (2004).

- [31] Grajski Kamil A., Tseng Ryan and Wheatley Chuck, “Loosely coupled wireless power transfer: Physics, circuits, standards”, *IEEE International Microwave Workshop Series on Innovative Wireless Power Transmission, Kyoto, Japan*, pp.1202-1208, May 2012.
- [32] T. Thabet and J. Woods, “An Approach to Calculate the Efficiency for an N-Receiver Wireless Power Transfer System”, (*IJACSA*) *International Journal of Advanced Computer Science and Applications*, Vol. 6, No. 9, 2015.
- [33] A. Furuya¹, Y. Uehara¹, K. Shimizu¹, J. Fujisaki¹, T. Ataka¹, T. Tanaka and H. Oshima, “Magnetic Field Analysis for Dimensional Resonance in Mn-Zn Ferrite Toroidal Core and Comparison with Permeability Measurement,” *IEEE Transactions on Magnetics*, Vol. 53, No. 1, 2016.



CIRRUCILUM VITAE

Name : Khalid Waleed Hussein AL-HASHEMI
Date of Birth : 27/03/1982
Title : Senior Engineer.
Address : 505-30-32/1, Baghdad, Iraq
Tel : +9647901280806
Email : khalidele@yahoo.com



EDUCATION

High School : Markaziyah High School, Baghdad, Iraq, 2000.
Undergraduate : Electrical Engineering Department, College of Engineering, Al-Mustansiriya University, Baghdad, Iraq, 2005.
Graduate : Electrical and Electronics Engineering Department, University of Turkish Aeronautical Association, Ankara, Turkey, 2017.

WORK EXPERIENCE

Iraqi ministry of electricity / Energy Distribution Office, since 2008
Specialize: In high voltage and low voltage network design.